2019-03

Modeling transmission dynamics and control of anthrax

Efraim, Joely E

NM-AIST

https://doi.org/10.58694/20.500.12479/2483

MODELING TRANSMISSION DYNAMICS AND CONTROL OF ANTHRAX

Joely Ezekiely Efraim

A Dissertation Submitted in Partial Fulfillment of the Requirements for the Degree of Master's in Mathematical and Computer Sciences and Engineering of the Nelson Mandela African Institution of Science and Technology

Arusha, Tanzania

March, 2019

ABSTRACT

Anthrax is a zoonotic disease caused by Bacillus anthraces. In this study the deterministic mathematical models for transmission dynamics of anthrax in absence and presence of control strategies in humans and animals are presented and analyzed to determine which parameters are sensitive to the disease and how will control strategies help to eradicate the disease. Using normalized sensitivity index, sensitivity index of each parameter with respect to basic reproduction number R_0 is derived and find that, parameters such as anthrax transmission's rate β, animal's recruitment rate b_a, animal's natural death rate, and pathogen's natural death rate are most sensitive to the transmission dynamics of anthrax. Stability analysis for equilibrium states by linearization, Metzler matrix, and Lyapunov function shows that the disease-free equilibrium is locally and globally asymptotically stable when $R_0 < 1$ and endemic equilibrium is globally asymptotically stable when $R_0 > 1$. The analysis shows that when free pathogens are destroyed with fumigants both susceptible humans and animals flourish while infected humans and animals decrease. It is also found that pathogens and carcasses decrease due to the fumigation effect. The analysis also shows that when carcasses are incinerated and removed from the affected area both humans and animals increase while infected humans and animals decrease. The analysis also shows that incineration and complete removal of carcasses makes the population of carcasses and pathogens decrease. The study also found that when all control strategies such as fumigation, incineration and complete removal of carcasses, animal's treatment, and humans treatment are all administered both susceptible humans and animals increase, infected humans and animals decrease and carcasses and pathogens decrease.

DECLARATION

I, Joely Ezekiely Efraim, do hereby declare to the Senate of Nelson Mandela African Institution of Science and Technology that this dissertation is my own original work and that it has neither been submitted nor presented for similar a award in any other institution.

Joely Ezekiely Efraim (Candidate)	Date

The above declaration is confirmed

Prof. Dmitry Kuznetsov (Supervisor 1)	Date
 Dr. Jacob Ismail Irunde (Supervisor 2)	Date

COPYRIGHT

CERTIFICATION

The undersigned certify that they have read and hereby recommend for acceptance by the Nelson Mandela African Institution of Science and Technology the dissertation entitled: Modeling Transmission Dynamics and Control of Anthrax, in fulfillment of the requirements for the degree of Masters in Mathematical and Computer Sciences and Engineering of the Nelson Mandela African Institution of Science and Technology.

Prof. Dmitry Kuznetsov
(Supervisor 1)

Date: .....

Dr. Jacob Ismail Irunde
(Supervisor 2)

Date: .....

ACKNOWLEDGMENT

First I very humbly thank my Lord, Almighty God by granting this very rare opportunity to join the Master's program at the Nelson Mandela African Institution of Science and Technology (NM-AIST). Secondly, I express sincere thanks to my supervisors Prof. Dmitry Kuznetsov, Dr. Jacob Ismail Irunde for dedicating their time to make this research successfully since without their support this work could not be possible. I do thanks also our late Dr. Yaw Nkansah Gyekye for his constructive and valuable contribution during proposal development and its defense. Also, I thank Prof. Elifuraha Gerad Mtalo, Dr. Dina Machuve, Dr. Shubi Kaijage, Dr. Musa Dida, Prof. Verdiana Masanja and the School of COCSE for their valuable contribution to this work. On top of that, I am indebted to the whole community of the NM-AIST for their support during the whole time of my study. My special thanks go to my employer University of Bagamoyo (UOB) for releasing me to pursue my studies and my sponsor Germany Academic Exchange (DAAD) for their financial support because without their support it could not be possible to pursue my studies. I also thank my family, my brothers Lukas Ezekiely, Noely Ezekiely and beloved sisters Upendo Ezekiely and Ester Ezekiely) for their love, encouragement during the whole journey of my studies. Lastly, I thank classmates Ivy Bimbiga, Florence Magoyo, Fred Kapange, Fikiri Matonya, Mfano Charles, Fabius Alfred, Saidy Raphely and my PhD colleagues Linus Kisoma, Annodi Mwapinga and Musa Antidius Mjankwi for their constructive criticism and valuable contributions during the coursework, proposal development, and dissertation writing. Lastly, may our living God bless you all, amen.

DEDICATION

I dedicate this work to my family.

TABLE OF CONTENTS

LIST OF TABLES

LIST OF FIGURES

ABBREVIATIONS

DFE	Disease Free Equilibrium
EE	Endemic Equlibrium
R_0	Basic Reproduction number
R_e	Effective Reproduction number
NM-AIST	The Nelson Mandela Institution of Science and Technology
C.D.C.P	Centre for Disease and Prevention
O.E	Organization and Epizootic
COCSE	Communication and Computational Science and Engineering
ODE	Ordinary Differential Equation

LIST OF APPENDICES

CHAPTER ONE

INTRODUCTION

1.1 Background Information

Anthrax is an acute infectious disease caused by a bacterium called Bacillus anthraces (Mushayabasa *et al.*, 2015). The disease is transmitted in four different forms that include, inhalation, ingestion, contact, and injection. Herbivorous are more vulnerable to infection when they eat sufficient spores in the soil or on plants (Turnbull, 2002). Omnivorous as well are vulnerable to the disease and they catch the infection through eating meat which is contaminated with anthrax. There are four forms of anthrax disease which are inhalation, ingestion or gastrointestinal, injection and cutaneous anthrax disease (for Animal Health, 2008). Inhalational anthrax infections have a higher mortality compared to another type of infection. This is because its diagnosis can sometimes be delayed since early indicators of the disease is similar to flu-like and sometimes it can be overlooked by medical personnel (Day *et al.*, 2011). The disease is easily transmitted from animals to humans (for Animal Health, 2008). Therefore, there is a great need of conducting further research on anthrax since it has become an epidemic.

1.1.1 Cutaneous anthrax

Cutaneous anthrax is one of the forms of anthrax which occurs when anthrax spores get into the skin, usually through a cut or scrape. This can happen when a person handles the infected animal's or contaminated animal's products like wool, hides or hair. This form of anthrax is illustrated in Fig. 1 where we see pathogens get into a human body via a cut or wound. This form of anthrax differs from other types on its mode of transmission where it is transmitted via the skin opening such as scrape or wounds. It is most prevalent among human beings. It has been reported that Arusha and Kilimanjaro are the most affected areas of this form of anthrax (Mwakapeje *et al.*, 2018). Its symptoms include a raised, itchy bump resembling an insect bite that quickly develops into a painless sore with a black center. Also, it is associated with swelling in the sore and nearby lymph glands (for Animal Health, 2008).

Figure 1: This figure shows the cutaneous type of anthrax (for Animal Health, 2008)

1.1.2 Gastrointestinal anthrax

Gastrointestinal anthrax is a rare but serious bacterial disease. It is one of the three main types of anthrax. A person can acquire it from eating meat which is infected with bacillus anthraces bacteria or their spores. Also, herbivores for instance cattle can get the disease during grazing when they eat contaminated grasses. Antibiotics, vaccination and supportive treatment can cure the disease, though, it results in death for 25 to 60 percent of all cases. This type or form of anthrax is also demonstrated in Figure 2. Here It is seeing that a human being is eating an infected meat.

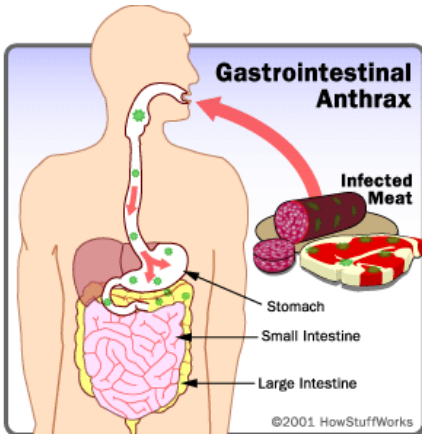

Figure 2: Gastrointestinal anthrax (for Animal Health, 2008)

1.1.3 Injection Anthrax

Recently, another type of anthrax infection has been identified as a heroin-injecting drug user in northern Europe. Symptoms of injection anthrax may be similar to those of cutaneous anthrax. Symptoms of injection anthrax may be infection deep under the skin or in the muscle where

the drug was injected. Injection anthrax can spread throughout the body faster and be harder to recognize and treat .

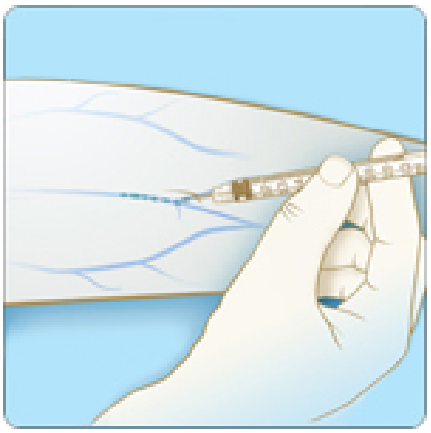

Figure 3: This figure shows the injectional type of anthrax (for Animal Health, 2008)

1.1.4 Inhalation Anthrax

Inhalation anthrax is the most deadly way to contract the disease, it is often fatal or deadly. The symptoms for inhalation anthrax include flu-like such as a sore throat, mild fever, fatigue, and muscle aches and mild chest and discomfort (Sinkie and Murthy, 2016).

1.1.5 The Cycle Infection of Anthrax Disease

Figure 4 shows the cycle of anthrax between animal (cattle) and human. Spores (spores forming bacillus anthraces) are the central point of the cycle, though, vegetative-forms also play an important role in introducing infection. For instance, human and carnivores can eat animal's meat that died of anthrax (for Animal Health, 2008). The cycle of infection stipulated above describes two modes of transmission that is by vector or by contact. Our study considers transmission by contact because other modes have been studied (Mushayabasa *et al.*, 2015).

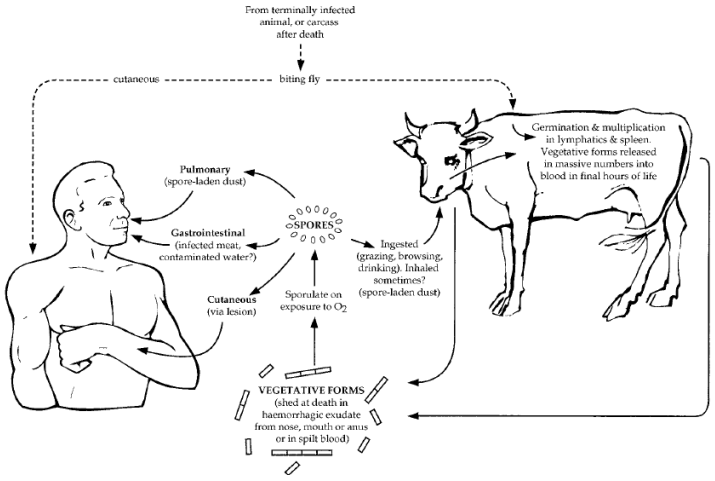

Figure 4: The Cycle Infection of Anthrax Disease, (for Animal Health, 2008)

Anthrax is a serious disease since its discovery in the 1870's. Grasses serve as exploited habitats of Bacillus anthracis and grazing animals such as sheep, goat, and cattle which are predominantly victims (Raymond *et al.*, 2010). The alkaline soil with a pH greater than 6.0, high nitrogen level caused by decaying vegetation in the soil, balanced periods of rain, droughts, and temperature higher than 15 degrees Celsius facilitate the occurrence of this disease (Mourez *et al.*, 2002). Anthrax has persisted in Africa where for example in Kruger National Park in South of Africa, the number of roan antelope declined from 450 to 45 animals (Harrington *et al.*, 1999).

In Tanzania, 109 Black Wildebeest, 21 Grant's gazelle,10 cattle and 26 goats died (Lembo *et al.*, 2011). Also in the Kilimanjaro region, 36 people were hospitalized after eating the meat of a contaminated cow (Mwakapeje *et al.*, 2018). In Arusha as well it has been reported that out of 134 infected people 8 died due to anthrax. Also, in Dar es, Salaam out of 22 people 6 died due to anthrax infections (Mwakapeje *et al.*, 2018).

1.2 Problem Statement

Anthrax is one of the diseases which affect both animals and human being. Though there are few mathematical models which study the transmission dynamics of anthrax and its control strategies, there are few and almost none of mathematical models that has considered the interaction between infected animals, carcasses, pathogen's reservoir (environment) and humans. This study is conducted to study transmission dynamics of anthrax when animals, carcasses, pathogen's reservoir and human beings are collectively considered. The controls strategies such as incineration, fumigation, treatment, disinfection and decontamination are considered to

conclude how the disease can be controlled.

1.3 Research Objectives

1.3.1 General Objective

The general objective of the study was to develop and analyze a mathematical model for the transmission dynamics and control of anthrax.

1.3.2 Specific Objectives

i. To formulate a mathematical model for the transmission dynamics of Anthrax.

ii. To compute reproduction number and determine which parameter is sensitive to the disease.

iii. To derive equilibrium points and analyze their stability.

iv. To examine the impact of control strategies.

1.4 Research Questions

This research intended to answer the following questions:

i. How can a mathematical model for the dynamics of anthrax be formulated?

ii. Which state variables and parameters can be included to make the model meaningful?

iii. How can equilibrium points be derived?

iv. What impact do control strategies have on dynamics of anthrax?

1.5 Significance of the Research

The transmission dynamics of anthrax is quite complicated and its outbreak can occur due to daily activities such as physical contact, ingestion, inhalation, therefore it is important to develop a mathematical model that explains and predicts the transmission dynamics of the disease and assists public health planning for the better way of eradicating the disease. The findings of this study will help to:

i. Create awareness about how anthrax is transmitted and what are risk factors.

ii. Design and implement the suggested control such as disinfection, early treatment, decontamination, fumigation and incineration for the eradication of the disease.

iii. The study will also motivate the application of mathematical models to study real-world problems.

CHAPTER TWO

LITERATURE REVIEW

A number of studies on transmission dynamics of anthrax have been conducted. Day *et al.* (2011) developed a mathematical model that describes the host (human) response to inhalation anthrax where they explored the early events of inhalation anthrax infection and possible points of intervention with respect to antibiotics. They developed a two-compartment model which comprises the lungs and the thoracic/mediastinal lymph nodes. The result revealed that, if the inhaled spore count is less than some critical threshold, then the infected individual will survive without treatment but above the threshold, the individual will die unless treated by the drug. However, the study found that, the initial number of spores is $2x10^4$ and treatment with Cipro or Doxy begins not later than 36 hours after exposure, the survival is possible but if the initial number of spores is $2x10^7$, then the death is imminent even if the treatment starts 12 hours after exposure, however, the study did not include human beings in the transmission dynamics of anthrax.

Friedman and Yakubu (2013) extended an anthrax epizootic model developed by Hahn and Furniss (1983). They investigated the effects of carcasses ingestion, carcasses induced environmental pollution and carcass removal in animals population for anthrax transmission. On carcasses, the study found that as carcasses are eliminated in the game reserves the number of animals which die from anthrax decreases. However, the study did not look at the transmission of anthrax from infected animals to humans when they interact with the fact that the disease is zoonotic.

Mushayabasa *et al.* (2015) developed a mathematical model that explores the spread of anthrax in herbivorous animals, whereby in their model, they have incorporated the components such as fast and slow progression of carcass disposal and vector population. The output of the model suggested that carcass disposal may have significantly reduced the spread of anthrax in animal's surrounding. This research proposes to develop the mathematical model that will explore more about the spread and dynamics of this disease between animals and human beings.

Sinkie and Murthy (2016) developed a mathematical model for anthrax in animal population by modifying the model which was developed by Mushayabasa *et al.* (2015). The study concluded that increasing the treatment rate and proper management of carcasses decreases pathogens and increases susceptible animals.

Saad-Roy *et al.* (2017) formulated a mathematical model for the same disease where they included live animals, infected carcasses and spores in the environment. They computed the basic

reproduction number (R_0) and establish that unique endemic equilibrium exists when the basic reproduction number R_0 is greater than one. From their findings, they deduced that when herbivorous alone are included the disease is eradicated if $R_0 < 1$.The study also found oscillatory solution from Hopf bifurcations (Guckenheimer *et al.*, 1997) where numerical results show existence of Hopf bifurcation for a certain parameter values when $R_0 > 1$.

Osman *et al.* (2018) developed a very current mathematical model that explains the transmission dynamics of anthrax between humans and vector population. They revealed that when recovering of human and animal decreases the basic reproduction number increases. Though this study was done parallel to this study but there is a quit difference since it wasn't considered the environment as the main source of infection. Not only that but also it wasn't considered the carcass population in anthrax transmission.

After reviewing of some of the literature as discussed above, we concluded that none of the studies considered transmission dynamics of anthrax between humans, animal, carcasses and pathogen's reservoir (environment), therefore our study intends to formulate a mathematical model that fills this gap.

CHAPTER THREE

MATERIALS AND METHODS

This chapter describes various methods, materials, and techniques that have been used in this study. It also presents an analysis of the invariant regions, basic and effective reproduction numbers and finally the stability analysis.

3.1 Materials and Methods

The study used SICP (Susceptible-Infected-Carcass-Pathogen) compartments and differential equation in developing the deterministic models for the dynamics of anthrax among and between humans and animals. The next generation matrix operator is used to compute the basic and effective reproduction numbers. Linearization method and Roth-Hurwitz criterion are used to prove the stability analysis of equilibrium points. Linearization method is the process of finding the linear approximation to a function at a given point. In a dynamical system, linearization is used in assessing the local stability of an equilibrium point of a system of nonlinear differential equations or discrete dynamical systems. Maximum Likelihood Estimator (MLE) is used in parameters estimation. Maximum Likelihood Estimator is a statical method used to estimate population parameters such as mean and variance. It can be also used by Epidemiologists to estimate a parameter that can best fit the trend of real data collected together with theoretical data obtained from the theoretical model's solutions for the purpose of prediction. In the side of materials, the study used MATLAB for numerical simulation, MAPLE for analytical analysis and R-Statistics for statical analysis.

Table 1 shows, in summary, the stated objectives and the corresponding methods to accomplish the objectives.

Table 1: Summary of Objectives and Methods

Objectives	**Methods**
To formulate a mathematical model for the transmission dynamics of anthrax.	The Ordinary differential equations are used to formulate the transmission dynamics model of anthrax.
To compute reproduction number and determine which parameter is sensitive to the disease.	The next generation matrix operator is used to compute the basic reproduction number.
To derive equilibrium points and analyze their stability.	Linearization method and Roth-Hurwitz criterion are used to determine the local stability of the disease-free equilibrium.
To determine how control strategies affect the dynamics.	All of the above three methods are used

3.2 Model Development

The model for anthrax is formulated by extending the models which were developed by Mushayabasa *et al.* (2015) and Sinkie and Murthy (2016) to include human beings. Dynamics of anthrax divides human and animal population each into two classes: susceptible S_h and infected I_h humans, and susceptible S_a and infected I_a animals respectively. Carcasses' class is represented by C.

Susceptible humans increase due to birth at a rate b_h and decrease due to anthrax infection after eating meat from infected animal and carcasses at a rate σ. They also acquire the disease when they eat or comes into contact with infected carcasses at a rate of δ and when they come into contact with an environment which is contaminated with pathogen at a rate ϕ. However, infected humans increase at a rate of σ when susceptible human eat meat from infected animal and carcasses. They also increase when the susceptible human eats or come into contact with infected carcasses at a rate δ and when they come into contact with the environment which is contaminated with pathogens at a rate of ϕ. However, infected humans decrease due to anthrax and natural induced deaths at rates r and μ_h respectively.

Susceptible animals replenish due to birth at a rate b_a and decrease due to anthrax infection following contact with pathogens at a rate β. Infected animals increase following infection of

the susceptible animal at a rate β, they suffer disease induced death at a rate of π. All animal classes suffer natural mortality at a rate of μ_a.

Carcasses increase when infected animals die due to anthrax at a rate π due to anthrax-induced death rate and decrease due to decomposition at a rate of θ and shed pathogens to the environment at the same rate. The pathogens increase at a rate of θ following carcass's decomposition and decrease at a rate of ω due to natural death and sometimes due to rain flushing. The interaction between infected animals, the environment, and humans is illustrated in Fig. 5.

3.3 Model Assumptions

The following are the model assumptions:

i. All animals and human are susceptible

ii. The recruitment rate of a new individual is through birth and immigration

iii. No incubation period in both animals and humans because the infection's period is very small

iv. All susceptible individuals are equally likely to be infected.

v. Animals and humans in each compartment have natural death rate μ_a and μ_h respectively.

vi. Infected animals and environment (pathogen's reservoir) are the main sources of anthrax infection.

vii. The pathogens are shed to the environment when carcasses are decomposed.

3.4 Model Flow Diagram

The model flow diagram is illustrated in Fig. 5.

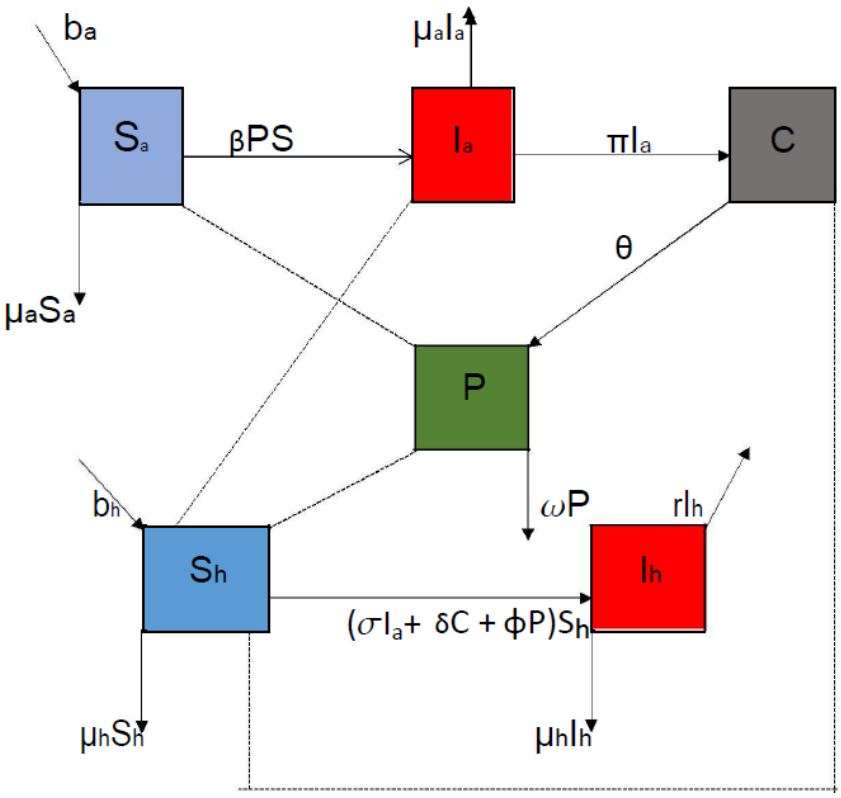

Figure 5: Model flow diagram

3.5 Model Variables Description

Variables for the model 3.1 are described in Table 2.

Table 2: Model Variables Description

Symbol	Description
$S_a(t)$	Susceptible animal at time t. t
$S_h(t)$	Susceptible human at time t.
$I_a(t)$	Infected animal at time t.
$I_h(t)$	Infected human at time t.
$C(t)$	Carcass population at time t.
$P(t)$	Population of pathogens in the environment at time t

3.6 Parameters' Descriptions

The parameters for model 3.1 are described in Table 3.

Table 3: Parameters' Descriptions

Parameter	Descriptions
b_a	Recruitment rate for animals
β	Anthrax transmission rate to animals.
σ	Anthrax transmission rate from an infected animal to human beings.
δ	Anthrax transmission rate from carcasses to human beings.
ϕ	Anthrax transmission rate from the environment to human beings
μ_a	Animal natural death rate
μ_h	Human natural death rate
σ	Contact rate between human and infected animals
b_h	Recruitment rate of human
θ	Pathogens shedding rate from carcasses to the environment
π	Animal's death rate due to anthrax
r	Human's death rate due anthrax

3.7 Model Equations

Putting all formulations together, we have the following system of equations:

$$\frac{dS_h}{dt} = b_h - (\sigma I_h + \delta C + \phi P + \mu_h)S_h, \tag{3.1a}$$

$$\frac{dI_h}{dt} = (\sigma I_a + \delta C + \phi P)S_h - (\mu_h + r)I_h, \tag{3.1b}$$

$$\frac{dP}{dt} = \theta C - \omega P, \tag{3.1c}$$

$$\frac{dS_a}{dt} = b_a - (\beta P + \mu_a)S_a, \tag{3.1d}$$

$$\frac{dI_a}{dt} = \beta P S_a - (\mu_a + \pi)I_a, \tag{3.1e}$$

$$\frac{dC}{dt} = \pi I_a - \theta C. \tag{3.1f}$$

$S_h(0) > 0; I_h(0) \geq 0; P(0) \geq 0; S_a(0) > 0; I_a(0) \geq 0; C(0) \geq 0.$

3.8 Model Properties

To analyze the model, it is important to determine whether the model is mathematically meaningful. The model is meaningful both biologically and mathematically if the solutions are positive and they are bounded. Boundedness and positivity of solutions are determined in the next section.

3.8.1 Invariant Region

The invariant region shows the boundedness of solutions. To determine the invariant we consider the population of human, animals, and pathogens separately. To come up with the invariant region where the solution of the model system (3.1) is feasible, we adopt the method used by Mushayabasa *et al.* (2015) and Irunde *et al.* (2016). The populations of humans, animals, and pathogens are denoted by N_h, N_a and P respectively. Human population is given by:

$$N_h = S_h + I_h.$$

$$\frac{dN_h}{dt} \leq b_h - \mu_h S_h. \tag{3.2}$$

Solving the inequality (3.2) we get:

$$N_h(t) \leq \frac{b_h}{\mu_h} + \left(N_h(0) - \frac{b_h}{\mu_h}\right) e^{-\mu_h t}. \tag{3.3}$$

but as t tends to infinity then: $N_h \leq \frac{b_h}{\mu_h}$ for $N_h(0) = S_h(0) + I_h(0)$.
For animal population:

$$N_a = S_a + I_a + C, \tag{3.4}$$

$$\frac{dNa}{dt} \leq b_a - \mu_a N_a. \tag{3.5}$$

Therefore the solution is given by:

$$N_a(t) \leq \frac{b_a}{\mu_a} + \left(N_a(0) - \frac{b_a}{\mu_a}\right) e^{-\mu_a t}. \tag{3.6}$$

For $N_a(0) = S_a(0) + I_a(0) + C(0)$
Analysis of solution (3.6) considers two cases:
When $N_a(0) \geq \frac{b_a}{\mu_a}$ and $N_a(0) \leq \frac{b_a}{\mu_a}$. When $N_a(0) \geq \frac{b_a}{\mu_a}$

$$N_a(t) \leq \frac{b_a}{\mu_a} + \left(N_a(0) - \frac{b_a}{\mu_a}\right) e^{-\mu_a t}.$$

Since:

$$\lim_{t\to\infty} \left(N_a(0) - \frac{b_a}{\mu_a}\right) e^{-\mu_a t} \to \infty$$

,
then:

$$N_a(t) \leq \frac{b_a}{\mu_a}.$$

From the definition of N_a it follows that:

$$\lim_{t\to\infty} S_a \leq \frac{b_a}{\mu_a} \lim_{t\to\infty} I_a \leq \frac{b_a}{\mu_a} \lim_{t\to\infty} C \leq \frac{b_a}{\mu_a}.$$

For pathogen population we have:

$$\begin{aligned} \frac{dP}{dt} = \theta C - \omega P, \quad put \quad C \leq \frac{b_a}{\mu_a}, \\ \frac{dP}{dt} \leq \theta \frac{b_a}{\mu_a} - \omega P. \end{aligned} \tag{3.7}$$

Solving the inequality (3.7) we get:

$$P(t) = \theta \frac{b_a}{\omega \mu_a} + \left(P(0) - \theta \frac{b_a}{\omega \mu_a}\right) e^{\omega \mu_a t}. \tag{3.8}$$

Analysis of the solution (3.8) considers two cases, these are: $P(0) > \frac{\theta b_a}{\omega \mu_a}$ and $P(0) < \frac{\theta b_a}{\omega \mu_a}$.

When: $P(0) > \frac{\theta b_a}{\omega \mu_a}$

we have:

$$P(0) \leq \theta \frac{b_a}{\omega \mu_a} \leq \theta \frac{b_a}{\omega \mu_a} + \left(P(0) - \theta \frac{b_a}{\omega \mu_a} \right) e^{\omega t}$$

and when:

$$P(0) < \frac{\theta b_a}{\omega \mu_a},$$

we have:

$$P(0) \leq \theta \frac{b_a}{\omega \mu_a} \leq \theta \frac{b_a}{\omega \mu_a} + \left(P(0) - \theta \frac{b_a}{\omega \mu_a} \right) e^{\omega t}.$$

Since:

$$\left(P(0) - \theta \frac{b_a}{\omega \mu_a} \right) e^{-\omega t} \to 0$$

then:

$$\lim_{t \to \infty} P < \frac{b_a}{\omega \mu_a}.$$

Therefore the model system (3.1) is positive invariant in the region:
$\Gamma = \{(S_a, I_a, C, P, S_h, I_h) \in R_+^6 : 0 \leq S_a + I_a + C \leq \frac{b_a}{\mu_a}, 0 \leq P \leq \theta \frac{b_a}{\omega \mu_a}, 0 \leq S_h + I_h \leq \frac{b_h}{\mu_h}\}$.
Solution for the model system (3.1) which begins on the boundary of the boundary region Γ converge to the region and remain bounded. Therefore the model (3.1) is mathematically and epidemiologically meaningful and we can consider flow generated for analysis. This result is summarized in the following theorem;

Theorem 1: *Solutions of the model system* (3.1) *enter the region:*

$$\Gamma = \{(S_a, I_a, C, P, S_h, I_h) \in R_+^6 : 0 \leq S_a + I_a + C \leq \frac{b_a}{\mu_a}, 0 \leq P \leq \theta \frac{b_a}{\omega \mu_a}, 0 \leq S_h + I_h \leq \frac{b_h}{\mu_h}\}. \tag{3.9}$$

3.8.2 Positivity of Solutions

Theorem 2: *Let the initial value of variables of the model* (3.1) *be* $S_a(0) > 0, I_a(0) > 0, P(0) > 0, C(0) > 0, S_h(0) > 0$ *and* $I_h(0) > 0$. *Then the solution set* $\Gamma = \{S_a(0) > 0, I_a(0) > 0, P(0) > 0, C(0) > 0, S_h(0) > 0, I_h(0) > 0\}$ *is positive for all time t.*

Proof: Lets consider the equation number (3.1a) of the model system (3.1), we have:

$$\begin{aligned} \frac{dS_a}{dt} &= b_a - (\beta P + \mu_a) S_a, \\ \frac{dS_a}{dt} &\geq -(\beta P + \mu_a) S_a, \end{aligned} \tag{3.10}$$

By separating variables we get:

$$\frac{dS_a}{S_a} \geq -(\beta P + \mu_a) dt, \tag{3.11}$$

By integrating both sides, we get:

$$\begin{aligned} \int \frac{dS_a}{S_a} &\geq \int_0^t (\beta P + \mu_a) dt, \\ \ln S_a &\geq -\int_0^t (\beta P + \mu_a) dt + C, \\ S_a(t) &\geq e^{\int_0^t -(\beta P + \mu_a) t}. \end{aligned} \tag{3.12}$$

At initial condition, we get:

$$\begin{aligned} S_a(t) &\geq S_a(0) e^{\int_0^t (\beta P(s) + \mu_a) dt}, \\ S_a(t) &\geq S_a(0) e^{\int_0^t (\beta P(s) + \mu_a) dt}. \end{aligned} \tag{3.13}$$

Then, $S_a(t) \geq 0, \forall\, t \geq 0$.

From the equation number (3.1b) of the model (3.1) we have:

$$\begin{aligned} \frac{dI_a}{dt} &= \beta P S_a - (\mu_a + \pi) I_a, \\ \frac{dI_a}{dt} &\geq -(\mu_a + \pi), \\ \frac{dI_a}{I_a} &\geq -(\mu_a + \pi) dt, \\ \int \frac{dI_a}{I_a} &\geq -\int_0^t (\mu_a + \pi) dt, \\ I_a(t) &\geq I_a(0) e^{-(\mu_a + \pi) t} \geq 0. \end{aligned} \tag{3.14}$$

From the equation (3.1c) of the model (3.1), we have:

$$\begin{aligned} \frac{dC}{dt} &= \pi I_a - \theta C, \\ \frac{dC}{dt} &\geq -\theta C, \\ \int \frac{dC}{C} &= -\int_0^t \theta dt, \\ C(t) &\geq C(0) e^{-\theta t} \geq 0. \end{aligned} \tag{3.15}$$

From the equation number (3.1d) of the model (3.1), we have:

$$\begin{aligned} \frac{dP}{dt} &= \theta C - \omega P, \\ \frac{dP}{dt} &\geq -\omega P, \\ \frac{dP}{P} &= \int_0^t -\omega dt. \end{aligned} \tag{3.16}$$

Solving (3.16) we get:
$P(t) \geq P(0)e^{-\omega t} \geq 0.$

Again from the equation (3.1e) of the model 3.1, we have:

$$\begin{aligned} \frac{dS_h}{dt} &= b_h - (\sigma I_h + \delta C + \mu_h + \phi P)S_h, \\ \int \frac{dS_h}{S_h} &\geq -\int_0^t (\sigma I_h + \delta C + \mu_h + \phi P)dt, \\ S_h(t) &\geq S_h(0)e^{-\int_0^t (\sigma I_h + \delta C + \mu_h + \phi P)dt} \geq 0. \end{aligned} \tag{3.17}$$

From the equation number (3.1f) of the model (3.1), we have:

$$\begin{aligned} \frac{dI_h}{dt} &= (\sigma I_h + \delta C + \phi P)S_h - (\mu_h + r)I_h, \\ \frac{dI_h}{dt} &\geq -(\mu_h + r)I_h, \\ \int \frac{dI_h}{I_h} &= \int_0^t -(\mu_h + r)dt, \\ I_h t \geq I_h(0)e^{-(\mu_h + r)t} &\geq 0. \end{aligned} \tag{3.18}$$

3.9 Model Analysis

In this section, we derive the equilibrium states and determine their stability. We start with disease-free equilibrium and conclude with endemic equilibrium.

3.10 The Basic Reproduction Number R_0

The basic reproduction number is the average number of secondary infections generated by a single infective individual when introduced in an entirely susceptible population (Diekmann *et al.*, 1990; Irunde *et al.*, 2016). Basic reproduction number R_0 determines whether the disease

persists or clears out. The disease clears out when $R_0 < 1$ and persists when $R_0 > 1$ (Irunde *et al.*, 2016). To compute the basic reproduction number R_0, we adopt the next generation matrix method where new infections and transfer terms are considered. If the new infections are mathematically defined by f_i and transfer terms by v_i, then the matrices F and V are given by:

$$F = \frac{\partial f_i}{\partial X_j}(x_0) \ \ and \ \ V = \frac{\partial v_i}{\partial X_j}(x_0). \tag{3.19}$$

as defined by Van den Driessche and Watmough (2002) . The basic reproduction number is therefore given by $R_0 = \rho(FV^{-1})$. From the model equations, the new infections and transfer terms are given by,

$$f_i = \begin{bmatrix} (\sigma I_a + \delta C + \phi P)S_h \\ 0 \\ \beta P S_a \\ 0 \end{bmatrix}. \tag{3.20}$$

and;

$$v_i = \begin{bmatrix} (\mu_h + r)I_h \\ \theta C - \omega P \\ (\mu_a + \pi)I_a \\ \pi I_a - \theta C \end{bmatrix}. \tag{3.21}$$

Derivatives of f_i and v_i with respect to infected classes at disease-free equilibrium point are:

$$F = \begin{bmatrix} 0 & \sigma\frac{b_h}{mu_h} & \delta\frac{b_h}{\mu_h} & \phi\frac{b_h}{\mu_h} \\ 0 & 0 & 0 & 0 \\ 0 & \beta\frac{b_a}{\mu_a} & 0 & 0 \\ 0 & 0 & 0 & 0 \end{bmatrix}. \tag{3.22}$$

and

$$V = \begin{bmatrix} \mu_h + r & 0 & 0 & 0 \\ 0 & -\omega & 0 & \theta \\ 0 & 0 & \mu_a + \pi & 0 \\ & 0 & 0 & \pi & -\theta \end{bmatrix}. \tag{3.23}$$

The inverse of the matrix V is:

$$V^{-1} = \begin{bmatrix} \frac{1}{\mu_h + r} & 0 & 0 & 0 \\ 0 & \frac{-1}{\omega} & \frac{\pi}{(\mu_a+\pi)\omega} & \frac{-1}{\omega} \\ 0 & 0 & \left(\frac{1}{\mu_a+\pi}\right) & 0 \\ 0 & 0 & \frac{\pi}{(\mu_a+\pi)\theta} & \frac{-1}{\theta} \end{bmatrix}. \tag{3.24}$$

and the product of matrices F and V^{-1} is;

$$FV^{-1} = \begin{bmatrix} 0 & -\frac{\phi\, b_h}{\mu_h \omega} & \frac{\sigma\, b_h}{\mu_h(\mu_a+\pi)} + \frac{\delta\, b_h \pi}{\mu_h(\mu_a+\pi)\theta} + \frac{\phi\, b_h \pi}{\mu_h(\mu_a+\pi)\omega} & -\frac{\delta\, b_h}{\mu_h \theta} - \frac{\phi\, b_h}{\mu_h \omega} \\ 0 & 0 & 0 & 0 \\ 0 & -\frac{\beta\, b_a}{\omega\, \mu_a} & \frac{\pi\, \beta\, b_a}{\mu_a(\mu_a+\pi)\omega} & -\frac{\beta\, b_a}{\omega\, \mu_a} \\ 0 & 0 & 0 & 0 \end{bmatrix}. \tag{3.25}$$

Therefore the basic reproduction number R_0 is given by:

$$R_0 = \frac{\beta b_a \pi}{\mu_a(\mu_a + \pi)\omega}. \tag{3.26}$$

The results show that the basic reproduction number R_0 depends on infection rate between animals and free pathogens β, animal's recruitment rate b_a, animal's death rate due to anthrax π, animal's natural death rate μ_a and pathogen's natural death rate ω. The parameters β and b_a are directly proportional to R_0, therefore increasing these parameters will also increase basic reproduction number R_0. Parameters μ_a and ω which are animal and pathogens natural death rate respectively are inversely proportional to R_0

3.11 Sensitivity Analysis

Sensitivity analysis assists to understand the potentials of each parameter to disease transmission (Hamby, 1994). It identifies sensitive parameters which should be the target when designing disease interventions. We employ the Maximum Likelihood estimation, and inbuilt Matlab fminsearch function to estimate parameters.

Table 6 shows the model parameter values. Parameter values from the related literature were used as initial values to fit the model from the data collected from the field. The data were collected at Ngorongoro district in Tanzania from 2006 to 2016 (Mwakapeje *et al.*, 2018).

3.12 Parameter Estimation

Ordinary differential equations (ODEs) are widely used in epidemiology to describes the dynamical behaviour of systems of interacting populations. However, ODEs rarely provide quantitative solutions that are close to real field observations or experimental data because natural systems are often subject to environmental noise and epidemiologists are often uncertain about the correct parameterization (Romero-Campero *et al.*, 2008; Myung, 2003).

Once a model is specified with its parameters and data has been collected, one is in a position to evaluate its goodness of fit, that is, how well it fits the observed data. The goodness of fits is assessed by finding parameter values of a model that best fits the data (Myung, 2003). The Documentary review is used to gather data in this study. There are two general methods of parameter estimation. These are Least Square Estimation (LSE) and Maximum Likelihood Estimation (MLE). Maximum Likelihood Estimation is a standard approach to parameter estimation since it has many optimal properties such as sufficient and efficient. The efficient means lowest possible variance of parameter estimates achieved asymptotically. LSE method is not considered as a general method for parameter estimation, but rather as an approach that is primarily used with linear regression models. The idea of MLE is to maximize the likelihood function. In this work, we used a sum of squares of residuals (SSR) defined as:

$$L(\theta) = \sum_{i=1}^{N} (Y_i - Y_i^{estimated})^2. \tag{3.27}$$

The equation (3.27) is used to find the optimal parameters by minimizing $L(\theta)$. The $\{y_i\}_{i=1}^{N}$ is a set of real data and $\{y_i^{estimated}{}_{i=1}^{N}\}$ is the solution of ODE at a given parameter value and θ is a vector of unknown parameters. Having $L(\theta)$, a built in MATLAB optimizer called fminsearch is used to obtain optimal parameters. Table 6 shows the estimated parameters values against literature and assumed values. The solution of the ODE 3.1 using estimated parameters in Table 6 fits the model as shown in Figure 10. Also the trend of both anthrax in humans and animal is illustrated by Fig. 8

3.13 Sensitivity Analysis of Reproduction Number R_0

In this section parameters' indices with respect to basic reproduction number, R_0 are determined. The basic reproduction number R_0 depends on five parameters which are used to derive an analytical expression for each parameter. If λ is a parameter in the basic reproduction number R_0 its sensitivity index with respect to R_0 is given by:

$$r_{\lambda}^{R_0} = \frac{\partial R_0}{\partial \lambda} x \frac{R_0}{\lambda}. \tag{3.28}$$

Using equation (3.28), sensitivity index for each parameter is given in Table 4. Here, the sensitivity analysis is done using estimated parameters.The sensitivity analysis reveals that parameters such as anthrax transmission rate β,animal recruitment rate b_a, animal natural death rate μ and free pathogens natural death rate ω are the most sensitive parameters to the basic reproduction number while anthrax induced rate π, is less sensitive as it is shown in Table 4.

Table 4: Sensitivity Indices

Parameter	Sensitivity Index
β	$+1.0000$
b_a	$+1.0000$
π	$+0.0014$
μ_a	-1.0014
ω	-1.0000

3.14 Equilibrium States and Stability Analysis

In this sub-section, stability analysis and equilibrium points are well discussed. The free and endemic equilibrium points are computed. Also, local and global stability is proved. We employed the linearization method to analyze and prove the local stability of free equilibrium point of our basic model 3.1. Also, we used the method used by Castillo-Chavez (2002) to prove the global stability of free equilibrium point.

3.14.1 Disease Free Equilibrium Point

The disease-free equilibrium point (DFE) is the state when there is no disease. We adopted the method of next generation used by Mushayabasa *et al.* (2015) and (Irunde *et al.*, 2016) to find the disease-free equilibrium point. We obtain disease free equilibrium when: $\frac{dS_a}{dt} = \frac{dI_a}{dt} = \frac{dC}{dt} = \frac{dP}{dt} = \frac{dS_h}{dt} = \frac{dI_h}{dt} = 0$ and $N_a = S_a$ and $N_h = S_h$. In this state, both animal and human population remain susceptible to the disease. At disease equilibrium point equations, the system (3.1) reduces to:

$$\begin{aligned} b_a - \mu_a S_a = 0, \\ b_h - \mu_h = 0. \end{aligned} \tag{3.29}$$

respectively whose solutions are $S_a = \frac{b_a}{\mu_a}$ and $S_h = \frac{b_h}{\mu_h}$ respectively.
Therefore disease free equilibrium is given by:

$$E^0(S_a, I_a, C, P, S_h, I_h) = \left(\frac{b_a}{\mu_a}, 0, 0, 0, \frac{b_h}{\mu_h}, 0\right). \tag{3.30}$$

3.15 Stability Analysis of the Disease Free Equilibrium (DFE)

Both local and global stability analyses are discussed in this section. We begin with local stability and concludes with global stability.

3.15.1 Local Stability of Disease Free equilibrium

The local stability of the disease equilibrium is analyzed by the method used by Mushayabasa *et al.* (2015). We conclude local stability when the Jacobian matrix at disease-free equilibrium has negative eigenvalues or eigenvalues have negative real parts. To study the local stability of diseases free equilibrium using the linearization method, we state and prove the following theorem:

Theorem 3: *The disease-free equilibrium Eo is locally asymptotically stable if* $R_0 < 1$ *and unstable if* $R_0 > 1$.

Proof: We linearize the model at disease-free equilibrium to obtain the matrix:

$$J_{E^o} = \begin{bmatrix} -\mu_h & 0 & -\frac{\phi\, b_h}{\mu_h} & 0 & -\frac{\sigma\, b_h}{\mu_h} & -\frac{\delta\, b_h}{\mu_h} \\ 0 & -\mu_h - r & \frac{\phi\, b_h}{\mu_h} & 0 & \frac{\sigma\, b_h}{\mu_h} & \frac{\delta\, b_h}{\mu_h} \\ 0 & 0 & -\omega & 0 & 0 & \theta \\ 0 & 0 & -\frac{\beta\, b_a}{\mu_a} & -\mu_a & 0 & 0 \\ 0 & 0 & \frac{\beta\, b_a}{\mu_a} & 0 & -\mu_a - \pi & 0 \\ 0 & 0 & 0 & 0 & \pi & -\theta \end{bmatrix}. \tag{3.31}$$

Disease-free equilibrium is locally asymptotically stable if all eigenvalues are negative. Eigenvalues in the first, second and fourth columns are $\mu_h, -(\mu_h + r)$ and $-\mu_a$ respectively.

The matrix (3.31) now reduces to 3x3 matrix.

$$J_{E^o} = \begin{bmatrix} -\omega & 0 & \theta \\ \frac{\beta\, b_a}{\mu_a} & -\mu_a - \pi & 0 \\ 0 & \pi & -\theta \end{bmatrix}. \tag{3.32}$$

whose characteristic equation is:

$$\lambda^3 + (\omega + \mu_a + \pi + \theta)\lambda^2 + (\omega\pi + \pi\theta + \omega\theta + \omega\mu_a + \theta\mu_a)\lambda - \frac{\theta\left(\beta\pi b_a - \omega\pi\mu_a - \omega{\mu_a}^2\right)}{\mu_a}. \tag{3.33}$$

The coefficients $a_1 > 0$ and $a_2 > 0$ since all parameters are positive.
However, $a_3 > 0$ if and only if

$$\frac{\theta\left(-\beta\pi b_a + \omega\pi\mu_a + \omega{\mu_a}^2\right)}{\mu_a} > 0. \tag{3.34}$$

Simplifying equation (3.34), we have:

$$\frac{\theta\beta\pi b_a}{\mu_a}\left(\frac{\omega(\pi+\mu_a)\mu_a}{\beta\pi b_a} - 1\right) > 0. \tag{3.35}$$

Now, the inequality (3.35) is positive if;

$$\left(\frac{\omega(\pi+\mu_a)\mu_a}{\beta\pi b_a} - 1\right) > 0, \tag{3.36}$$

$$\frac{1}{R_0} - 1 > 0, \tag{3.37}$$

$$R_0 < 1. \tag{3.38}$$

According to Routh-Hurwitz criteria, all eigenvalues have negative real parts if $R_0 < 1$, disease-free equilibrium is locally asymptotically stable when $R_0 < 1$. This result is summarized in the following theorem:
Theorem 4: *The disease-free equilibrium for model* (3.1) *is locally asymptotically stable when* $R_0 < 1$.

3.15.2 Global stability of Disease Free Equilibrium

Equilibrium states are said to be stable if all solutions remain close to equilibrium point for all time. To determine the global stability of disease-free equilibrium, we adopt the method used by Castillo-Chavez (2002). Using the method, system (3.1) is written as:

$$\begin{aligned} \frac{dX_n}{dt} &= C(X_n - X_{dfe}) + C_1 X_i, \\ \frac{dX_i}{dt} &= C_2 X_i. \end{aligned} \tag{3.39}$$

where X_n represents non-transmitting classes, X_i represents transmitting classes and X_{dfe} represents disease free equilibrium respectively. C, C_1 and C_2 are matrices to be obtained from

system (3.39). Global stability is proved if eigenvalues of matrix C are negative and C_2 is Metzler matrix defined mathematically as $C_2(x_{ij}) \geq 0 \; \forall i \neq j$.

Adopting the system in equation (3.39), the system (3.1) is written as:

$$\begin{pmatrix} b_h - (\sigma I_a + \delta C + \phi P + \mu_h) S_h \\ b_a - (\beta P + \mu_a) S_a \end{pmatrix} = C \begin{pmatrix} S_h - \dfrac{b_h}{\mu_h} \\ S_a - \dfrac{b_a}{\mu_a} \end{pmatrix} + C_1 \begin{pmatrix} I_h \\ P \\ I_a \\ C \end{pmatrix}. \tag{3.40}$$

and

$$\begin{pmatrix} (\sigma I_a + \delta C + \phi P) S_h - (\mu_h + r) I_h \\ \theta C - \omega P \\ \beta P S_a - (\mu_a + \pi) I_a \\ \pi I_a - \theta C \end{pmatrix} = C_2 \begin{pmatrix} I_h \\ P \\ I_a \\ C \end{pmatrix}. \tag{3.41}$$

Matrix C is 2×2 matrix which is

$$C = \begin{pmatrix} -\mu_h & 0 \\ 0 & -\mu_a \end{pmatrix}, \tag{3.42}$$

whose eigenvalues are $-\mu_a$ and $-\mu_h$. Matrix C_1 is 4×4 matrix given by:

$$\begin{pmatrix} 0 & -\phi \dfrac{b_h}{\mu_h} & -\sigma \dfrac{b_h}{\mu_h} & -\delta \dfrac{b_h}{\mu_h} \\ 0 & -\beta \dfrac{b_a}{\mu_a} & 0 & 0 \end{pmatrix}.$$

Matrix C_2 is also given by:

$$C_1 = \begin{pmatrix} -(\mu_h + r) & \phi \dfrac{b_h}{\mu_h} & \sigma \dfrac{b_h}{\mu_h} & \delta \dfrac{b_h}{\mu_h} \\ 0 & -\omega & 0 & \theta \\ 0 & \beta \dfrac{b_a}{\mu_a} & -(\mu_a + \pi) & 0 \\ 0 & 0 & \pi & -\pi \end{pmatrix}. \tag{3.43}$$

The diagonal elements of matrix (3.43) are negative while the off-diagonal elements are non-negative, hence it is a Metzler matrix. Hence proved.

3.16 Endemic Equilibrium

Endemic equilibrium refers to the state where the disease is prevalent in the population (Ugwa and Agwu, 2013). The existence of endemic equilibrium is illustrated by the Figure 6.

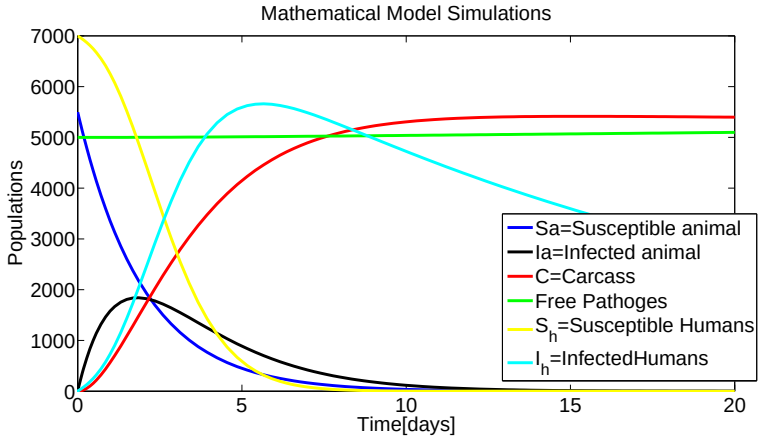

Figure 6: The existence of endemic equilibrium point

To determine how the epidemic interact with the hosts, we compute the endemic equilibrium. In this case, infected compartments are not zero that is $E^*(S_a^*, I_a*, C^*, P_*, S_h^*, I_h^*) \neq (0,0,0,0,0,0)$. Using the maple, the endemic equilibrium points are given as;
Let:

$$A = -b_h \theta \beta \omega \left(\mu_a + \pi\right)\left(\mu_h + r\right)$$

$$B = \mu_a \delta \left(\mu_a + \pi\right)\left(\mu_h + r\right)\omega^2 + \left(\phi\left(\mu_h + r\right)\mu_a - \beta\left(r\mu_h + \sigma b_h + {\mu_h}^2\right)\right)\left(\mu_a + \pi\right)\theta$$
$$- \delta b_a \left(\mu_h + r\right)\pi\beta\omega - \pi\phi\beta\theta b_a \left(\mu_h + r\right)$$

Then:

$$
\begin{aligned}
S_h^* &= -\frac{A}{B} \\
I_h^* &= \frac{b_h}{\mu_h + r} \\
P^* &= \frac{-\mu_a\left(\mu_a+\pi\right)\omega + \pi\,\beta\,b_a}{\beta\,\omega\,\left(\mu_a+\pi\right)} \\
P^* &= \mu_a\left(\frac{R_0}{\beta} - 1\right) \\
S_a^* &= \frac{\omega\,\left(\mu_a+\pi\right)}{\beta\,\pi} \\
S_a^* &= \frac{b_a}{\mu_a} R_0 \\
I_a^* &= \frac{\pi\,\beta\,b_a - \pi\,\omega\,\mu_a - \omega\,{\mu_a}^2}{\beta\,\left(\mu_a+\pi\right)\pi} \\
I_a^* &= \frac{\omega\mu_a}{\beta}\left(R_0 - \frac{1}{\pi}\right) \\
C^* &= \frac{\pi\,\beta\,b_a - \pi\,\omega\,\mu_a - \omega\,{\mu_a}^2}{\beta\,\left(\mu_a+\pi\right)\theta} \\
C^* &= (R_0 - 1)\frac{\omega\mu_a}{\beta\theta}
\end{aligned}
$$

3.16.1 Global Stability of Endemic Equilibrium

The stability analysis explains the behavior of the epidemic near the equilibrium points. The solutions which start near the equilibrium point and remain near for all times are stable solutions and represent a stable behavior of the epidemic. Solutions which converge to equilibrium point are asymptotically stable and they represent the asymptotically stable behavior of the epidemic (Irunde *et al.*, 2016).

$$Y(P) = a_1\left(S_h - S_h^* lnS_h\right) + a_2\left(I_h - I_h^* lnI_h\right) + a_3\left(P - P^* lnP\right) + a_4\left(S_a - S_a^* lnS_a\right) + a_5\left(I_a - I_a^* lnI_a\right) \tag{3.44}$$

$$+ a_6\left(C - C^* lnC\right), \tag{3.45}$$

where $a_i > 0$ for $i = 1, 2.....6..$ The derivative of Y is given by:

$$
\begin{aligned}
\frac{dY}{dt} = a_1\left(1 - \frac{S_h^*}{S_h}\right)\frac{dS_h}{dt} + a_2\left(1 - \frac{I_h^*}{I_h}\right)\frac{dI_h}{dt} + a_3\left(1 - \frac{P^*}{P}\right)\frac{dP}{dt} + a_4\left(1 - \frac{S_a^*}{S_a}\right)\frac{dS_a}{dt}, \\
+ a_5\left(1 - \frac{I_a^*}{I_a}\right)\frac{dI_a}{dt} + a_6\left(1 - \frac{C^*}{C}\right)\frac{dC}{dt},
\end{aligned}
\quad , \tag{3.46}
$$

and from (3.1) we have

$$\begin{aligned}\frac{dY}{dt} &= a_1\left(1-\frac{S_h^*}{S_h}\right)[b_h-(\sigma I_a+\delta C+\phi P+\mu_h)S_h]\\ &+a_2\left(1-\frac{I_h^*}{I_h}\right)[(\sigma I_a+\delta C+\phi P)S_h-(\mu_h+r)I_h],\\ &+a_3\left(1-\frac{P^*}{P}\right)[\theta C-\omega P]+a_4\left(1-\frac{S_a^*}{S_a}\right)[b_a-(\beta P+\mu_a)S_a]\\ &+a_5\left(1-\frac{I_a^*}{I_a}\right)[\beta P S_a-(\mu_a+\pi)I_a]\\ &+a_6\left(1-\frac{C^*}{C}\right)[\pi I_a-\theta C].\end{aligned} \tag{3.47}$$

At the endemic equilibrium point, equation (3.47) becomes;

$$\begin{aligned}\frac{dY}{dt} &= a_1\left(1-\frac{S_h^*}{S_h}\right)[(\sigma I_a+\delta C+\phi P+\mu_h)S_h^*-(\sigma I_h+\delta C+\phi P+\mu_h)S_h]\\ &+a_2\left(1-\frac{I_h^*}{I_h}\right)[(\mu_h+r)I_h^*],\\ &+a_3\left(1-\frac{P^*}{P}\right)[\omega P^*-\omega P]+a_4\left(1-\frac{S^*}{S_a}\right)[(\beta P+\mu_a)S_a^*-(\beta P+\mu_a)S_a]\\ &+a_5\left(1-\frac{I_a^*}{I_a}\right)[(\mu_a+\pi)I_a^*-(\mu_a+\pi)I_a],\\ &+a_6\left(1-\frac{C^*}{C}\right)[\theta C^*-\theta C].\end{aligned} \tag{3.48}$$

Rearrangement of terms and further simplification gives;

$$\begin{aligned}\frac{dY}{dt} &= -a_1\left(\frac{(S_h-S_h^*)^2}{S_h}\right)(\sigma I_h+\delta C+\phi P+\mu_h)-a_2\left(\frac{(I_h-I_h^*)^2}{I_h}\right)(\mu_h+\pi)-a_3\frac{(P-P^*)^2}{P}\omega,\\ &+a_4\left(\frac{(S_a-S_a^*)^2}{S_a}\right)(\beta P+\mu_a)-a_5\left(\frac{(I_a-I_a^*)^2}{I_a}\right)(\mu_a+\pi)-a_6\left(\frac{(C-C^*)^2}{C}\right)\theta+F(\Gamma).\end{aligned} \tag{3.49}$$

where

$$\Gamma=(S_h,I_h,P,S_a,I_a,C)>0$$

, and

$$F(\Gamma)=0.$$

According to Korobeinikov (2007) $F(\Gamma)$ is non-positive and therefore $F(\Gamma)\leq 0$ for all Γ. The derivative $\frac{dY}{dt}\leq 0$ in Γ, equality holds when $\Gamma=\Gamma^*$, since $\frac{dY}{dt}\leq 0$ for all Γ and $\frac{dY}{dt}=0$ when $\Gamma=\Gamma^*$, meaning that the largest invariant set in Γ when $\frac{dY}{dt}=0$ is singleton Γ which is the endemic equilibrium. Therefore, by LaSalle's invariance principle LaSalle (1976), it means

that endemic equilibrium point Γ^* is asymptotically stable in Γ when $R_{0T} > 1$. This result is summarized in the theorem 4.

Theorem 4:
Endemic equilibrium of the model system 3.1 is globally asymptotically stable when $R_{0T} > 1$ and it is globally asymptotically unstable otherwise.

3.17 The Model with Anthrax Control Strategies

In this section, we propose and discuss different control strategies in the dynamics of anthrax to determine if they can help to eradicate the disease. Dynamics of anthrax with animal and humans involves a cycle as described in Fig. 4. This study proposes the controls strategies such as disinfection, treatment, decontamination, fumigation, and incineration.

Decontamination of an animal product involves disposing of materials such as bedding, feedstuffs, manure, and incineration of carcasses (for Animal Health, 2008; Saad-Roy *et al.*, 2017). Disinfection involves the use of sporicides such as chlorine and formaldehyde which are made up of hydrogen peroxide. Fumigation as the control strategy involves the use of sporicidal fumigants such as formaldehyde, ethylene oxide, methyl bromide, hydrogen peroxides vapor and chlorine dioxide which are used in the infected areas (for Animal Health, 2008). Though researches have been conducted to study dynamics and control of anthrax in animals, no mathematical attention has been given to study the transmission dynamics of anthrax with controls when animal and human populations are considered. Therefore this study is using the mathematical technique to study the impact of control strategies in eradicating the disease.

3.18 Model Formulation

The model for anthrax is formulated by extending the models which were developed by Mushayabasa *et al.* (2015) and Sinkie and Murthy (2016) to include human beings. Dynamics of anthrax divides human and animal population each into two classes: susceptible S_h and infected I_h humans, and susceptible S_a and infected I_a animals respectively. Carcasses' class is represented by C.

Susceptible humans increase due to birth and recover when human beings are treated at rates b_h and k respectively. The class decreases due to anthrax infection after eating meat from infected animal and carcasses at a rate σ. They also acquire the disease when they eat or come into contact with infected carcasses and when they come into contact with an environment which is

contaminated with pathogen at rates δ and ϕ respectively.

However, infected humans increase at a rate σ when susceptible human eat meat from infected animal and carcasses. They also increase when the susceptible human eats or come into contact with infected carcasses and when they come into contact with an environment which is contaminated with pathogens at a rate of ϕ. However, they decrease due to recovery, anthrax and natural induced mortalities at rates k, r, and μ_h respectively.

Susceptible animals replenish due to birth and recovery of infected animals at rates b_a and γ respectively. However, they decrease due to infection following contact with pathogens at a rate of β. Infected animals increase following infection of the susceptible animal at a rate of β, they diminish due to disease-induced death and recovery after treatment at rates π and γ respectively. All animal classes suffer natural mortality at a rate of μ_a.

Infected animals die due to anthrax and become carcasses at a rate π. The Carcasses increase when infected animals die due to anthrax at a rate π increase at the rate of π due to anthrax-induced death rate and decrease due to decomposition, incineration removal at rates α and ζ and shed pathogens to the environment at a rate α. The pathogens increase at a rate of α following carcass's decomposition and decrease due to fumigation and natural death at rates Φ and ω respectively. The interaction between infected animals, environment, and humans under the control strategies is illustrated in Fig. 7.

3.19 Model Compartment

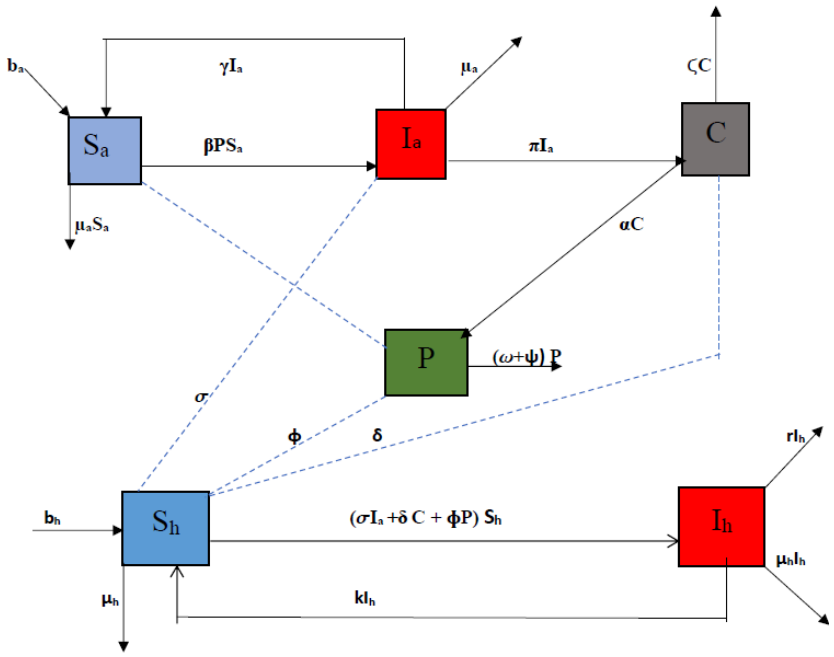

Figure 7: Interaction of animals and human in the presence of anthrax controls

3.20 Parameters' Description

The following are the model parameters:

Table 5: Parameters' Descriptions

Parameter	Descriptions
b_a	Recruitment rate for animals
β	Anthrax transmission rate to animals
σ	Anthrax transmission rate from an infected animal to human beings
δ	Anthrax transmission rate from carcasses to human beings
ϕ	Anthrax transmission rate from the environment to human beings
μ_a	Animal natural death rate
μ_h	Human natural death rate
σ	Contact rate between human and infected animals
b_h	Recruitment rate of human
α	Pathogens shedding rate from carcasses to the environment
π	Animal's death rate due to anthrax
r	Human's death rate due anthrax
k	The rate of treating infected humans
ζ	The rate of incinerating or burning and removing of carcasses
Ψ	The rate of applying fumigants to the pathogen's reservoir
γ	The rate of treating infected animals

3.21 Model Equations

$$\frac{dS_h}{dt} = b_h + kI_h - (\sigma I_h + \delta C + \phi P + \mu_h), \tag{3.50a}$$

$$\frac{dI_h}{dt} = (\sigma I_a + \delta C + \phi P)S_h - (\mu_h + r + k)I_h, \tag{3.50b}$$

$$\frac{dP}{dt} = \alpha C - (\omega + \Psi)P, \tag{3.50c}$$

$$\frac{dS_a}{dt} = b_a + \gamma I_a - (\beta P + \mu_a)S_a, \tag{3.50d}$$

$$\frac{dI_a}{dt} = \beta P S_a - (\mu_a + \pi + \gamma)I_a, \tag{3.50e}$$

$$\frac{dC}{dt} = \pi I_a - (\alpha + \zeta)C, \tag{3.50f}$$

subject to initial conditions $S_h(0) > 0; I_h(0) \geq 0; P(0) \geq 0; S_a(0) > 0; I_a(0) \geq 0; C(0) \geq 0$.

3.22 Model Analysis

3.22.1 Boundness of the Solution

To find the invariant region of the model system (3.50), we consider human population N_h, pathogens P and animal population N_a such that:
$N_h = S_h + I_h$ and $N_a = S_a + I_a + C$.

$$N_h = S_h + I_h, \tag{3.51}$$

$$\frac{dN_h}{dt} < b_h - \mu_h S_h, \tag{3.52}$$

Solving the inequality (3.52) we get:

$$N_h(t) \leq \frac{b_h}{\mu_h} + \left(N_h(0) - \frac{b_h}{\mu_h}\right) e^{-\mu_h t}. \tag{3.53}$$

but as t tends to infinity then: $N_h \leq \frac{b_h}{\mu_h}$ for $N_h(0) = S_h + I_h(0)$.
For animal population:

$$N_a = S_a + I_a + C, \tag{3.54}$$

$$\frac{dNa}{dt} \leq b_a - \mu_a N_a. \tag{3.55}$$

Therefore the solution is given by:

$$N_a \leq \frac{b_a}{\mu_a} + (N_a - \frac{b_a}{\mu_a}) e^{-\mu_a t}. \tag{3.56}$$

For $N_a(0) = S_a(0) + I_a(0) + C(0)$.
Analysis of solution (3.56) considers two cases:
When $N_a(0) \geq \dfrac{b_a}{\mu_a}$ and $N_a \leq \frac{b_a}{\mu_a}$,
and $N_a \leq \frac{b_a}{\mu_a} \leq \frac{b_a}{\mu_a} + (N_a(0) - \frac{b_a}{\mu_a}) e^{-\mu_a t}$,
Since; $\lim_{t\to\infty} (N_a(0) - \frac{b_a}{\mu_a}) e^{-\mu_a t} \to 0$,
$N_a \leq \frac{b_a}{\mu_a}$.
From the definition of N_a, it follows that; $\lim_{t\to\infty} S_a \leq \frac{b_a}{\mu_a}$, $\lim_{t\to\infty} I_a \leq \frac{b_a}{\mu_a}$, $\lim_{t\to\infty} C \leq \frac{b_a}{\mu_a}$.
For pathogen population we have:

$$\frac{dP}{dt} = \alpha C - (\Psi + \omega) P, \quad put \quad C \leq \frac{b_a}{\mu_a}, \tag{3.57}$$

$$\frac{dP}{dt} \leq \alpha \frac{b_a}{\mu_a} - (\Psi + \omega) P, \tag{3.58}$$

Solving the inequality (3.7) we get:

$$P(t) = \alpha \frac{b_a}{(\Psi + \omega)\mu_a} + (P(0) - \alpha \frac{b_a}{(\Psi + \omega)\mu_a}) e^{-(\omega + \Psi)\mu_a t}. \tag{3.59}$$

It follows that, analysis of the solution (3.59) considers two cases, these are;

$$P(0) > \alpha\frac{b_a}{(\omega+\Psi)\mu_a} \;\; ; \;\; P(0) \leq \alpha\frac{b_a}{(\omega+\Psi)\mu_a} \leq \alpha\frac{b_a}{(\omega+\Psi)\mu_a} + (P(0) - \tag{3.60}$$

$$\alpha\frac{b_a}{(\omega+\Psi)\mu_a})e^{-(\Psi+\omega)t}, \tag{3.61}$$

Since, $(P(0) - \alpha\frac{b_a}{(\omega+\Psi)\mu_a})e^{-(\omega+\Psi)t} \to 0$ then ; $\lim_{t\to\infty} P < \frac{b_a}{(\omega+\Psi)\mu_a}$,

Therefore the model system (3.50) is positive invariant in the region:

$$\Omega = \{(S_a, I_a, C, P, S_h, I_h) \in R_+^6 : 0 \leq S_a + I_a + C \leq \frac{b_a}{\mu_a}, 0 \leq P \leq \alpha\frac{b_a}{(\omega+\Psi)\mu_a}, 0 \leq S_h + I_h \leq \frac{b_h}{\mu_h}\}. \tag{3.62}$$

Solution for the model system (3.50) which begins on the boundary of the boundary region Ω converge to the region and it remains bounded. The of solutions in Ω hold. Therefore the model (3.50) is mathematically and epidemiologically meaningful and we can consider its analysis. This result is summarized in the following theorem;

Theorem 5: *Solutions of the model system* (3.50) *enter the region:*
$\Omega = \{(S_a, I_a, C, P, S_h, I_h) \in R_+^6 : 0 \leq S_a + I_a + C \leq \frac{b_a}{\mu_a}, 0 \leq P \leq \alpha\frac{b_a}{(\omega+\Psi)\mu_a}, 0 \leq S_h + I_h \leq \frac{b_h}{\mu_h}\}$.

3.22.2 The Effective Reproduction Number R_e

The anthrax average new infections when controls are implemented are measured by effective reproduction number R_e which is computed by next generation approach (Van den Driessche and Watmough, 2002). The control strategies are effective if $R_e < 1$ and ineffective if $R_e > 1$. Using the infected classes in the system (3.50), the vectors for new infection k_i and transfer terms t_j are:

$$k_i = \begin{bmatrix} (\sigma I_a + \delta C + \phi P)S_h \\ 0 \\ \beta P S_a \\ 0 \end{bmatrix}, \tag{3.63}$$

and

$$t_i = \begin{bmatrix} (\mu_h + r + k)I_h \\ \alpha C - (\omega+\Psi)P \\ (\mu_a + \pi + \gamma)I_a \\ \pi I_a - (\alpha+\zeta)C \end{bmatrix}. \tag{3.64}$$

The matrices **K** and **T** are therefore given by:

$$K = \begin{bmatrix} 0 & \sigma\frac{b_h}{mu_h} & \delta\frac{b_h}{\mu_h} & \phi\frac{b_h}{\mu_h} \\ 0 & 0 & 0 & 0 \\ 0 & \beta\frac{b_a}{\mu_a} & 0 & 0 \\ 0 & 0 & 0 & 0 \end{bmatrix}, \tag{3.65}$$

and

$$T = \begin{bmatrix} \mu_h + r + k & 0 & 0 & 0 \\ 0 & -(\omega + \Psi) & 0 & \theta \\ 0 & 0 & \mu_a + \pi + \gamma & 0 \\ 0 & 0 & \pi & -(\alpha + \varsigma) \end{bmatrix}, \tag{3.66}$$

and

$$T^{-1} = \begin{bmatrix} \frac{1}{(k+r+\mu_h)} & 0 & 0 & 0 \\ 0 & \frac{-1}{(\omega+\Psi)} & \frac{\theta\pi}{(\gamma+\mu_a+\pi)(\zeta+\alpha)(\omega+\Psi)} & -\frac{\alpha}{(\alpha+\zeta)(\omega+\Psi)} \\ 0 & 0 & \frac{1}{(\gamma+\mu_a+\pi)} & 0 \\ 0 & 0 & \frac{\pi}{(\gamma+\mu_a+\pi)(\zeta+\alpha)} & \frac{-1}{(\alpha+\zeta)} \end{bmatrix}. \tag{3.67}$$

The effective reproduction number, R_e is such that:

$$R_e = \rho(\mathbf{K}\mathbf{T}^{-1}). \tag{3.68}$$

We find that

$$R_e = \frac{\beta\, b_a \alpha\, \pi}{\mu_a\,(\gamma + \mu_a + \pi)\,(\alpha + \zeta)\,(\omega + \Psi)}. \tag{3.69}$$

The controls parameters such as rate of incinerating, removal and burial of carcasses, ζ and the rate of applying fumigants to the affected areas, Ψ are inversely proportional to the effective reproduction number. This implies that the increase of these parameters make the effective reproduction number to decrease.

3.23 Local Stability of a Disease Free Equilibrium

In this section linearization method is used to investigate the local stability of the disease free equilibrium. The model system (3.50) is linearized at a disease free equilibrium to obtain ma-

trix:

$$J(E^0) = \begin{bmatrix} -\mu_h & k & -\frac{\phi\, b_h}{\mu_h} & 0 & -\frac{\sigma\, b_h}{\mu_h} & -\frac{\delta\, b_h}{\mu_h} \\ 0 & -\mu_h - r - k & \frac{\phi\, b_h}{\mu_h} & 0 & \frac{\sigma\, b_h}{\mu_h} & \frac{\delta\, b_h}{\mu_h} \\ 0 & 0 & -\omega - \Psi & 0 & 0 & \alpha \\ 0 & 0 & -\frac{\beta\, b_a}{\mu_a} & -\mu_a & \gamma & 0 \\ 0 & 0 & \frac{\beta\, b_a}{\mu_a} & 0 & -\mu_a - \pi - \gamma & 0 \\ 0 & 0 & 0 & 0 & \pi & -\alpha - \zeta \end{bmatrix}. \tag{3.70}$$

The matrix $JE^(0)$ is locally asymptotically stable if all its eigenvalues are negative. From the first, second and fourth columns, the eigenvalues are $-\mu_h$, $-(\mu_h + r + k)$ and $-\mu_a$ respectively. The matrix (3.70) then reduces to:

$$\begin{bmatrix} -\omega - \Psi & 0 & \alpha \\ \frac{\beta\, b_a}{\mu_a} & -\mu_a - \pi - \gamma & 0 \\ 0 & \pi & -\alpha - \zeta \end{bmatrix}, \tag{3.71}$$

whose characteristic equation is:

$$\lambda^3 + b_2\lambda^2 + b_1\lambda + b_0.$$

where:

$$\begin{aligned} b_0 = {} & \frac{\pi\Psi\zeta\,\mu_a + \pi\Psi\alpha\,\mu_a + \pi\Psi\theta\,\mu_a + \pi\zeta\,\omega\,\mu_a + \pi\alpha\,\omega\,\mu_a - \pi\beta\,\theta\,b_a + \pi\,\omega\,\theta\,\mu_a}{\mu_a} \\ & + \frac{\Psi\zeta\,\gamma\mu_a + \Psi\zeta\,{\mu_a}^2 + \Psi\alpha\,\gamma\mu_a + \Psi\alpha\,{\mu_a}^2 + \Psi\gamma\alpha\,\mu_a + \Psi\alpha\,{\mu_a}^2 + (\zeta)\,\gamma\omega\,\mu_a}{\mu_a} \\ & + \frac{\zeta\,\omega\,{\mu_a}^2 + \alpha\,\gamma\omega\,\mu_a + \alpha\,\omega\,{\mu_a}^2 + \gamma\omega\,\alpha\,\mu_a + \omega\,\alpha\,{\mu_a}^2}{\mu_a}, \end{aligned}$$

$$\begin{aligned} b_1 = {} & (\pi\Psi + \pi\zeta + \pi\alpha + \pi\omega + \pi\theta + \zeta\Psi + \alpha\Psi + \Psi\gamma + \theta\Psi + \mu_a\Psi) \\ & + (\zeta\gamma + \zeta\omega + \zeta\mu_a + \alpha\gamma + \alpha\omega + \alpha\mu_a + \gamma\omega + \gamma\alpha + \alpha\omega + \mu_a\omega + \alpha\mu_a), \end{aligned}$$

$$b_2 = (\alpha + \zeta + \mu_a + \pi + \gamma + \omega + \Psi),$$

Using Hurwitz criterion, we can see that: $b_2 > 0$, $b_1 > 0$ but, $b_0 > 0$ if and only if,

$$b_0 = (\alpha+\zeta)(\omega+\Psi)(\mu_a+\pi+\gamma)\left[1-\frac{\pi\beta\alpha b_a}{(\theta+\alpha+\zeta)(\omega+\Psi)(\mu_a+\pi+\gamma)}\right] > 0, \tag{3.72}$$

$$= (\alpha+\zeta)(\omega+\Psi)(\mu_a+\pi+\gamma)(1-R_e) > 0. \tag{3.73}$$

Hence, $b_0 > 0$ if $R_e \leq 1$. According to Routh-Hurwitz criteria, all eigenvalues are negative or have negative real parts if $R_e < 1$. Therefore the disease free equilibrium is locally asymptotically stable when $R_e < 1$.

3.24 Global Stability of Disease Free Equilibrium

To establish the global stability of disease-free equilibrium, we adopt the method used by Castillo-Chavez (2002) and Irunde *et al.* (2016). Using this method, the system (3.50) can be written as:

$$\begin{aligned} \frac{dX_n}{dt} &= C(X_n - X_{dfe}) + C_1 X_i, \\ \frac{dX_i}{dt} &= C_2 X_i. \end{aligned} \tag{3.74}$$

where X_n represents non-transmitting classes, X_i represents transmitting classes and X_{dfe} stands for disease free equilibrium. C, C_1 and C_2 are matrices to be obtained from system (3.39). Global stability holds if eigenvalues of the matrix C are negative and C_2 is Metzler matrix defined mathematically as $C_2(x_{ij}) \geq 0 \; \forall i \neq j$. Adopting the form in equation (3.74), the system (3.50) is written as:

$$\begin{pmatrix} b_h + kI_h - (\sigma I_a + \delta C + \phi P + \mu_h)S_h \\ b_a + \gamma I_a - (\beta P + \mu_a)S_a \end{pmatrix} = C \begin{pmatrix} S_h - \dfrac{b_h}{\mu_h} \\ S_a - \dfrac{b_a}{\mu_a} \end{pmatrix} + C_1 \begin{pmatrix} I_h \\ P \\ I_a \\ C \end{pmatrix}, \tag{3.75}$$

and

$$\begin{pmatrix} (\sigma I_a + \delta C + \phi P)S_h - (\mu_h + r + k)I_h \\ \alpha C - (\omega + \Psi)P \\ \beta P S_a - (\mu_a + \pi + \gamma)I_a \\ \pi I_a - (\alpha + \zeta)C \end{pmatrix} = C_2 \begin{pmatrix} I_h \\ P \\ I_a \\ C \end{pmatrix}, \tag{3.76}$$

Matrix C is given by:

$$C = \begin{pmatrix} -\mu_h & 0 \\ 0 & -\mu_a \end{pmatrix}. \tag{3.77}$$

whose eigenvalues are: $-\mu_a$ and $-\mu_h$. Matrix C_1 is given by:

$$C_1 = \begin{pmatrix} k & -\phi\dfrac{b_h}{\mu_h} & -\sigma\dfrac{b_h}{\mu_h} & -\delta\dfrac{b_h}{\mu_h} \\ & & & \\ 0 & -\beta\dfrac{b_a}{\mu_a} & \gamma & 0 \end{pmatrix}. \tag{3.78}$$

Matrix C_2 is also given by:

$$\begin{pmatrix} -(\mu_h+r+k) & \phi\dfrac{b_h}{\mu_h} & \sigma\dfrac{b_h}{\mu_h} & \delta\dfrac{b_h}{\mu_h} \\ 0 & -(\omega+\Psi) & 0 & \alpha \\ 0 & \beta\dfrac{b_a}{\mu_a} & -(\mu_a+\pi+\gamma) & 0 \\ 0 & 0 & \pi & -(\alpha+\zeta) \end{pmatrix}. \tag{3.79}$$

Since the matrix (3.79) is a Metzler matrix and matrix (3.78) has negative eigenvalues, disease-free equilibrium is globally asymptotically stable.

3.25 Existence of Endemic Equilibrium

To compute endemic equilibrium, we employ maple software to obtain:

$$I_h^* = \frac{b_h}{\mu_h + r}. \tag{3.80}$$

$$P^* = \frac{-(\zeta+\alpha)(\omega+\Psi)\mu_a{}^2 - (\zeta+\alpha)(\omega+\Psi)(\gamma+\pi)\mu_a + \beta\,\pi\,\alpha\,b_a}{(\zeta+\alpha)(\mu_a+\pi)\beta\ (\omega+\Psi)}. \tag{3.81}$$

$$S_a^* = \frac{(\zeta+\alpha)(\omega+\Psi)(\pi+\gamma+\mu_a)}{\beta\,\pi\,\alpha} \tag{3.82}$$

$$= \frac{b_a}{R_e\mu_a}. \tag{3.83}$$

$$I_a^* = \frac{\beta\,\pi\,\alpha\,b_a - (\zeta+\alpha)(\omega+\Psi)\mu_a{}^2 - (\zeta+\alpha)(\omega+\Psi)(\gamma+\pi)\mu_a}{\pi\,(\mu_a+\pi)\beta\,\alpha} \tag{3.84}$$

$$C^* = \frac{-(\zeta+\alpha)(\omega+\Psi)\mu_a{}^2 - (\zeta+\alpha)(\omega+\Psi)(\gamma+\pi)\mu_a + \beta\,\pi\,\alpha\,b_a}{(\zeta+\alpha)(\mu_a+\pi)\beta\,\alpha}. \tag{3.85}$$

3.25.1 Global Stability of Endemic Equilibrium for Model With Control Strategies

The stability analysis explains more about the behavior of the epidemic near the equilibrium points. The solutions which start near the equilibrium point and remain near for all times are stable solutions and represent a stable behavior of the epidemic. Solutions which converge to equilibrium point are asymptotically stable and they represent the asymptotically stable behavior of the epidemic Irunde *et al.* (2016).

The global stability of the epidemic equilibrium is explored via the construction of a suitable Lyapunov function using Korobeinikov and Maini (2004). In this approach, Lyapunov function is constructed in the form of:

$$Y = \sum a_i \left(X_i - X_{i^*} lnX_i\right).$$

where a_i is properly selected constant, x_i is the population of the i^{th} compartment, and X^* is the equilibrium point. Therefore, consider the Lyapunov function:

$$V(P) = a_1\left(S_h - S_h^* lnS_h\right) + a_2\left(I_h - I_h^* lnI_h\right) + a_3\left(P - P^* lnP\right) + a_4\left(S_a - S_a^* lnS_a\right) \tag{3.86}$$

$$+ a_5\left(I_a - I_a^* lnI_a\right), + a_6\left(C - C^* lnC\right), \tag{3.87}$$

where $a_i > 0$ for $i = 1, 2.....6..$ The derivative of V is given by:

$$\begin{aligned} \frac{dV}{dt} &= a_1\left(1 - \frac{S_h^*}{S_h}\right)\frac{dS_h}{den} + a_2\left(1 - \frac{I_h^*}{I_h}\right)\frac{dI_h}{dt} + a_3\left(1 - \frac{P^*}{P}\right)\frac{dP}{dt} + a_4\left(1 - \frac{S_a^*}{S_a}\right)\frac{dS_a}{dt}, \\ &+ a_5\left(1 - \frac{I_a^*}{I_a}\right)\frac{dI_a}{dt} + a_6\left(1 - \frac{C^*}{C}\right)\frac{dC}{dt}, \end{aligned} \tag{3.88}$$

and from (3.50) we have

$$\begin{aligned} \frac{dV}{dt} &= a_1\left(1 - \frac{S_h^*}{S_h}\right)\left[b_h + kI_h - (\sigma I_a + \delta C + \phi P + \mu_h)S_h\right] \\ &+ a_2\left(1 - \frac{I_h^*}{I_h}\right)\left[(\sigma I_a + \delta C + \phi P)S_h - (\mu_h + r + k)I_h\right], \\ &+ a_3\left(1 - \frac{P^*}{P}\right)\left[\alpha C - (\omega + \Phi)P\right] \\ &+ a_4\left(1 - \frac{S_a^*}{S_a}\right)\left[b_a + \gamma - (\beta P + \mu_a)S_a\right] + a_5\left(1 - \frac{I_a^*}{I_a}\right)\left[\beta P S_a - (\mu_a + \pi + \gamma)I_a\right], \\ &+ a_6\left(1 - \frac{C^*}{C}\right)\left[\pi I_a - (\alpha + \zeta)C\right]. \end{aligned} \tag{3.89}$$

At the endemic equilibrium point, equation (3.47) becomes;

$$\begin{aligned}\frac{dY}{dt} &= a_1\left(1-\frac{S_h^*}{S_h}\right)[(\sigma I_a+\delta C+\phi P+\mu_h)S_h^*-(\sigma I_h+\delta C+\phi P+\mu_h)S_h]\\ &+a_2\left(1-\frac{I_h^*}{I_h}\right)[(\mu_h+r+k)I_h^*],\\ &+a_3\left(1-\frac{P^*}{P}\right)[(\omega+\Phi)P^*-(\omega+\Phi)P]\\ &+a_4\left(1-\frac{S^*}{S_a}\right)[(\beta P+\mu_a)S_a^*-(\beta P+\mu_a)S_a],\\ &+a_5\left(1-\frac{I_a^*}{I_a}\right)[(\mu_a+\pi+\gamma)I_a^*-(\mu_a+\pi+\gamma)I_a]\\ &+a_6\left(1-\frac{C^*}{C}\right)[(\alpha+\zeta)C^*-\theta C].\end{aligned} \tag{3.90}$$

Rearrangement of terms and further simplification gives;

$$\begin{aligned}\frac{dY}{dt} &= -a_1\left(\frac{(S_h-S_h^*)^2}{S_h}\right)(\sigma I_h+\delta C+\phi P+\mu_h)-a_2\left(\frac{(I_h-I_h^*)^2}{I_h}\right)(\mu_h+\pi+k)\\ &-a_3\frac{(P-P^*)^2}{P}(\omega+\zeta),\\ &+a_4\left(\frac{(S_a-S_a^*)^2}{S_a}\right)(\beta P+\mu_a)-a_5\left(\frac{(I_a-I_a^*)^2}{I_a}\right)(\mu_a+\pi+k)\\ &-a_6\left(\frac{(C-C^*)^2}{C}\right)(\zeta+\alpha)+F(\Gamma).\end{aligned} \tag{3.91}$$

where

$$\Gamma=(S_h,I_h,P,S_a,I_a,C)>0.$$

and

$$F(\Gamma)=0.$$

According to Korobeinikov (2007) $F(\Gamma)$ is non-positive and therefore $F(\Gamma)\leq 0$ for all Γ. The derivative $\frac{dY}{dt}\leq 0$ in Γ, equality holds when $\Gamma=\Gamma^*$, since $\frac{dY}{dt}\leq 0$ for all Γ and $\frac{dY}{dt}=0$ when $\Gamma=\Gamma^*$, meaning that the largest invariant set in Γ when $\frac{dY}{dt}=0$ is singleton Γ which is the endemic equilibrium. Therefore, by LaSalle's invariance principle LaSalle (1976), it means that endemic equilibrium point Γ^* is asymptotically stable in Γ when $R_{0T}>1$. This result is summarized in the theorem 5.

Theorem 6

Endemic equilibrium of the model system 3.1 is globally asymptotically stable when $R_{0T}>1$ and it is globally asymptotically unstable otherwise.

CHAPTER FOUR

RESULTS AND DISCUSSION

4.1 Introduction

In this chapter, we begin with numerical simulations where the model is fitted to data to obtain parameters which are then used in the simulation. The findings of the study are discussed in the next section.

4.2 Data Comparison to Model

Before fitting the model, we plot a bar chart to reveal the status of anthrax in both human and animals respectively. Figure 8 illustrates the anthrax trends in humans and animals. Figure 9 shows animal and human cases independently.

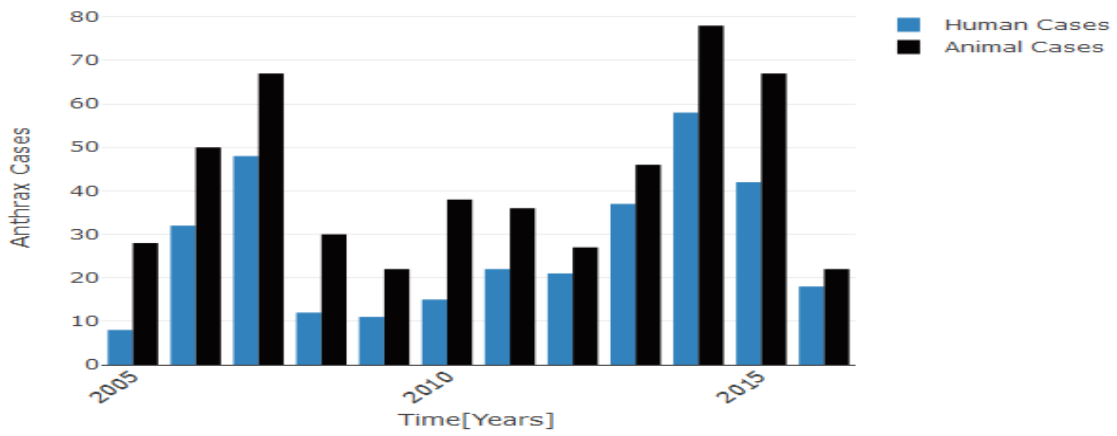

Figure 8: Trend of Anthrax for twelve years in Arusha and Kilimanjaro regions.

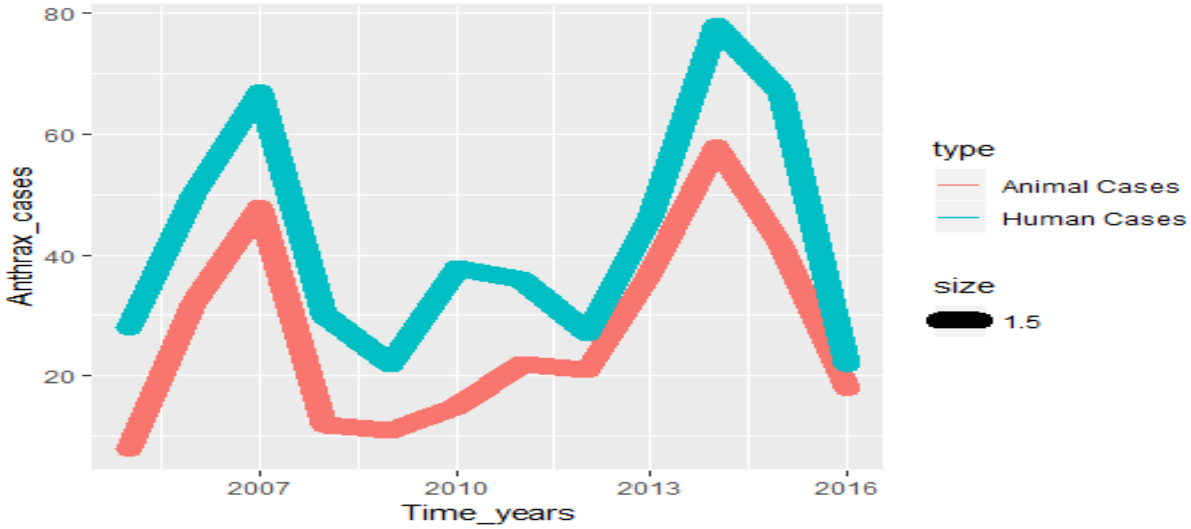

Figure 9: Trend of Anthrax for twelve years in Arusha and Kilimanjaro regions

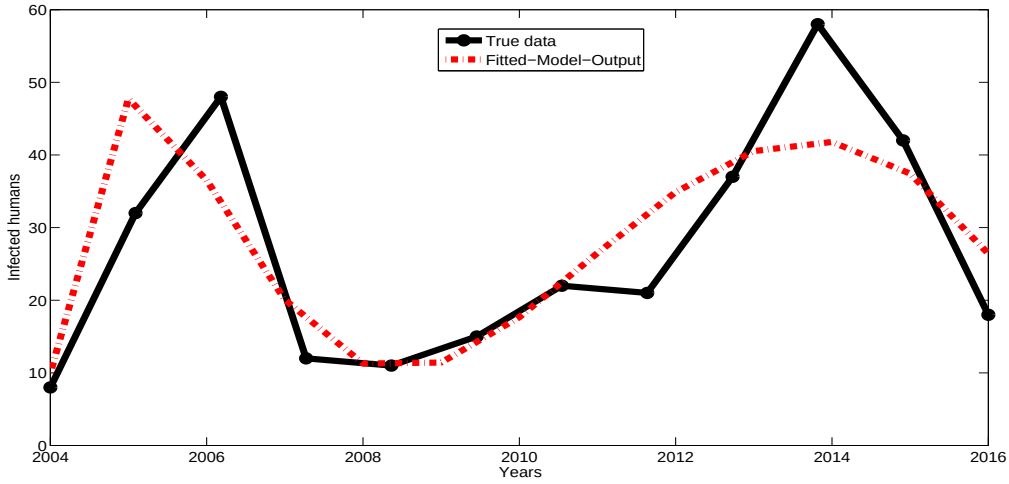

Figure 10: Model comparison with humans anthrax cases data

Figure 10 show how the model (3.1) is well compared with data collected from Arusha and Kilimanjaro regions Mwakapeje *et al.* (2018). The data were collected from 2004 to 2016. The black solid line shows the actual data and red grid line shows the solution of the model 3.1. The model follow the trend of data well for the given estimated parameter values. Parameters which are estimated from real data and the theoretical data are presented in the Table 6.

Table 6: Parameters Values

Parameter	Values &Units	Source	Estimated Parameters
b_a	$1.369 \times 10^{-}5\ \ day^{-1}$	Sinkie and Murthy (2016)	0.0002
β	$0.0001\ \ day^{-1}$	Sinkie and Murthy (2016)	0.0016
θ	$0.001125\ \ day^{-1}$	Sinkie and Murthy (2016)	0.0386
ω	$0.000014\ \ day^{-1}$	Sinkie and Murthy (2016)	0.0003
μ_a	$0.0001\ \ day^{-1}$	Sinkie and Murthy (2016)	0.0006
π	$0.06\ \ day^{-1}$	assumed	0.4141
μ_h	$0.00016\ \ day^{-1}$	assumed	0.0002
b_h	$0.015\ \ day^{-1}$	assumed	0.0005
δ	$0.000002\ \ day^{-1}$	Assumed	0.0001
ϕ	$0.000001219\ \ day^{-1}$	Assumed	0.0003

4.3 Numerical Simulation

We begin with the basic model by considering sensitive parameters and conclude with the model which has anthrax control strategies.

4.3.1 Numerical Simulation for Model without Controls

In this section, we analyze long and short terms behavior of anthrax dynamics in both humans and animal by considering sensitive parameters. To get a better understanding of anthrax transmission dynamics we use estimated parameters. The general dynamics of anthrax with no controls is demonstrated in Fig. 11.

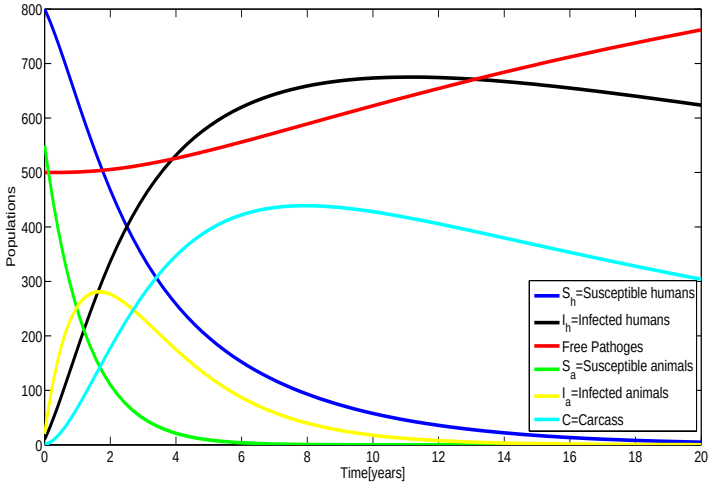

Figure 11: The general dynamics of anthrax in humans and animals

Susceptible humans and animals decrease exponentially due to the high rate of anthrax infection. Susceptible animals decrease as they acquire bacillus anthraces during grazing (Furniss and Hahn, 1981; for Animal Health, 2008). Susceptible humans decrease as they acquire anthrax from the environment or by eating meat from infected animals. The anthrax infection appears to be critical between five to fifteen years as demonstrated by Fig. 11. However, pathogens increase due to shedding and decomposition of carcasses.

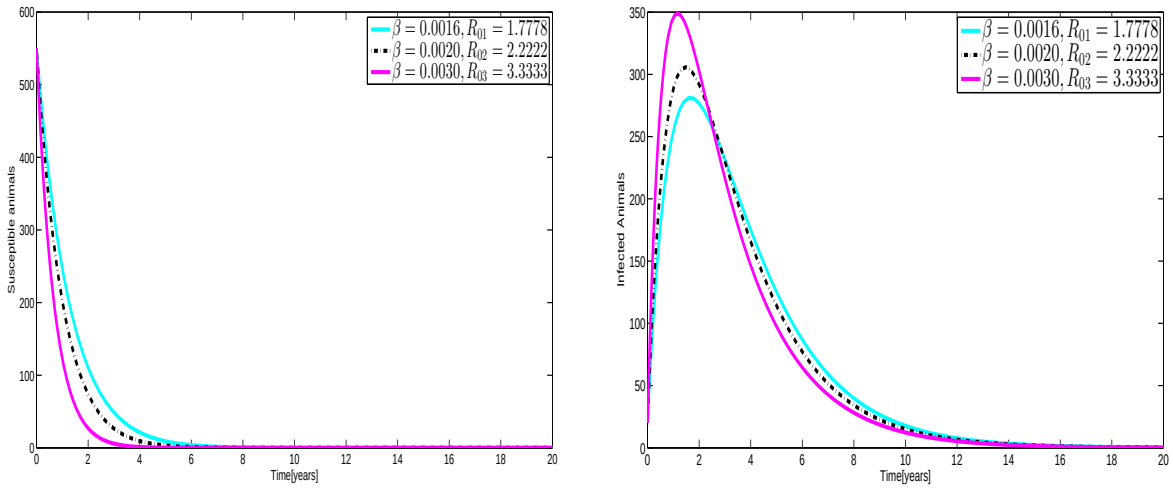

(a) Susceptible animals **(b)** Infected Animals

Figure 12: Variation of susceptible and infected animals with animal transmission rate

Figure 12 shows the effect of varying animal transmission rate to the dynamics of anthrax in both susceptible and infected animals. It is found that as the animal infection rate increases,

susceptible animals decrease while infected animals flourish. When animals are infected at a rate of 0.003 $year^{-1}$, all susceptible animals may acquire anthrax in fours years as demonstrated in Fig. 12a.

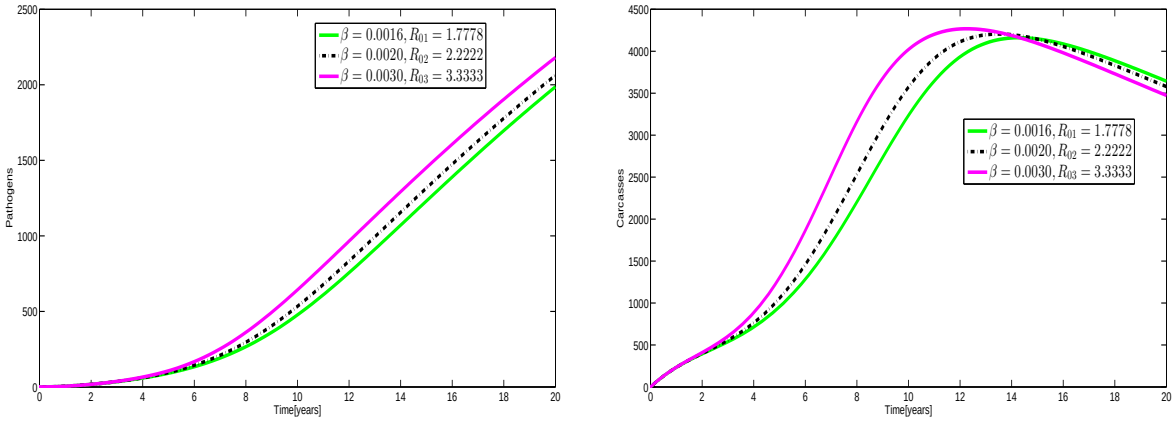

(a) Dynamics of anthrax in pathogens population **(b)** Anthrax in carcasses population

Figure 13: Variation of animal infection rate in carcass and pathogen Population

The Figure 13a shows the effect of varying animal transmission rate in both pathogens and carcasses population. The results show that as the animal transmission rate increases both carcasses and pathogens increase correspondingly.

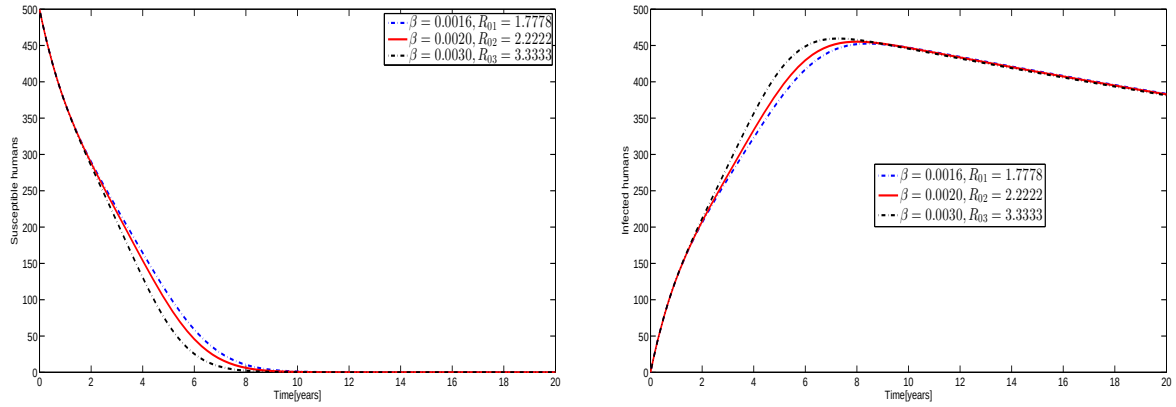

(a) Anthrax dynamics in susceptible humans **(b)** Anthrax dynamics in infected humans

Figure 14: Variation of animal infection rate in both susceptible and infected humans

Figure 14 shows the effect of varying animal transmission rate in both susceptible and infected humans. The results show that when the animal transmission rate increases, susceptible humans decrease. The rise and fall of the graph are due to the nature of the occurrence of the disease

whereby the disease erupts in seasonally during the rainy and high drought period.

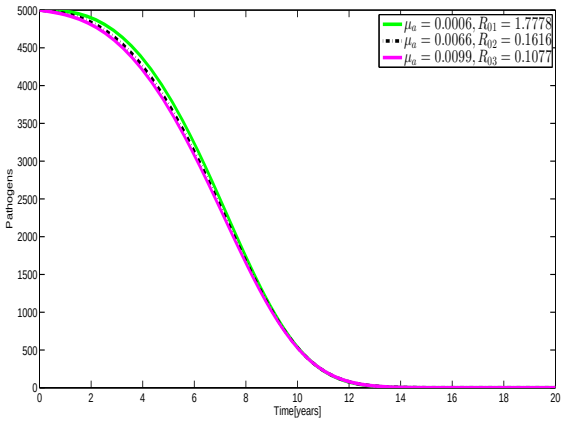

(a) Anthrax dynamics in pathogens population

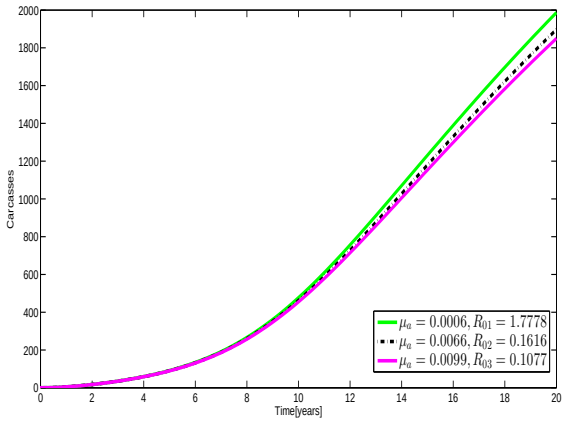

(b) Anthrax dynamics in carcasses population

Figure 15: Variation of animal natural death rate in both pathogens and carcasses

Figure 15 shows the effect of varying the animal natural death rate in both pathogens and carcasses population. The results show that when animal death rate increases both free pathogens and carcasses decreases. It is because animals play an important role in anthrax transmission.

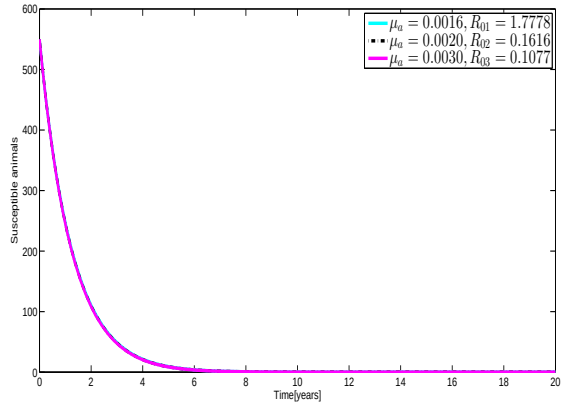

(a) Anthrax dynamics in susceptible animal population

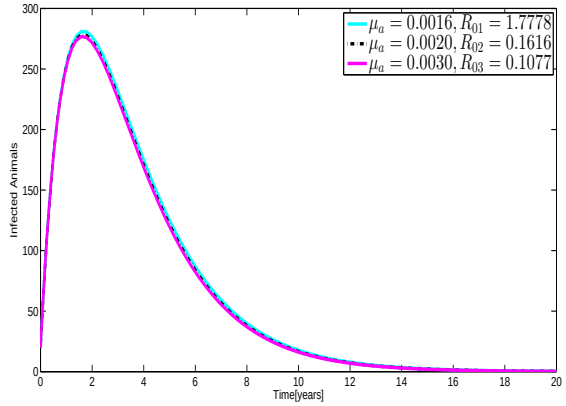

(b) Anthrax dynamics in infected animal population

Figure 16: Variation of animal natural death rate in both susceptible and infected animal

Figure 16 shows the effect of varying animal natural death rate in both infected and susceptible animals. The result shows that when the animal natural death rate increases both susceptible and infected animal decrease.

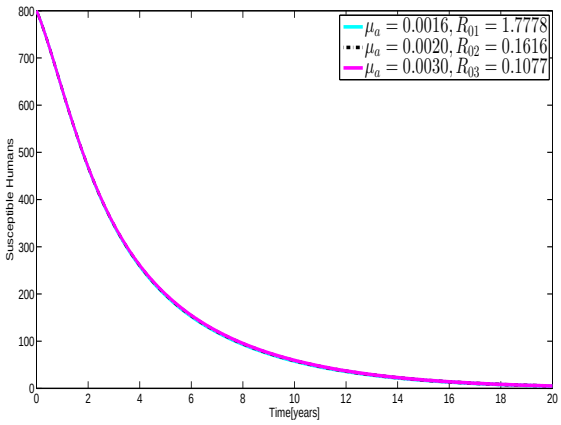

(a) Anthrax dynamics in susceptible humans

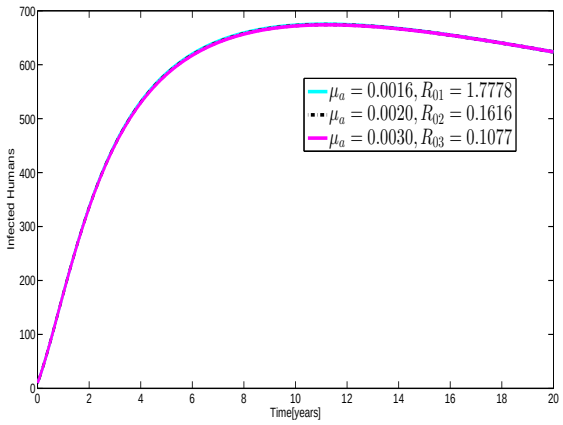

(b) Anthrax dynamics in infected humans

Figure 17: Variation of animal natural death rate in both susceptible and infected humans

Figure 17 shows the effect of varying animals natural death rate to both susceptible and infected humans. The results show that when animal natural death rate increases susceptible humane increases and infected humans decreases.

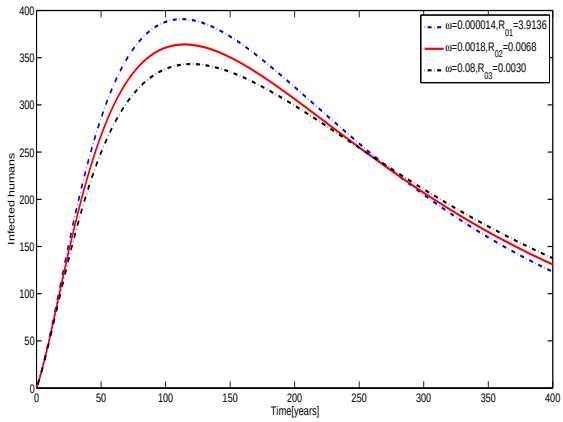

(a) Anthrax dynamics in susceptible humans

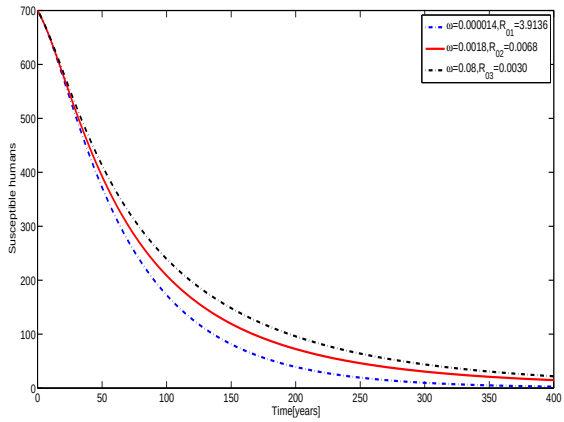

(b) Anthrax dynamics in infected humans

Figure 18: Variation of susceptible and infected humans with pathogen's death rate

In Fig. 18a, the results shows that when the natural death rate of pathogen increases, the human's infection ceases because pathogens are the source of infection to humans. In Fig. 18b, the increase in anthrax death rate ω, slow down the human's infection.

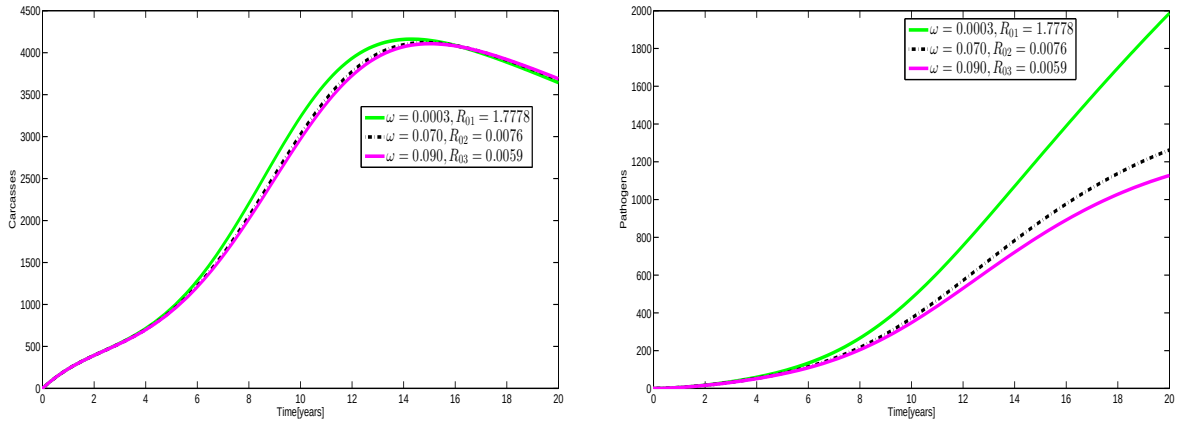

(a) Anthrax dynamics in carcasses **(b)** Anthrax dynamics in pathogen

Figure 19: The variation's effect of pathogen's natural death rate to the dynamics of both carcasses and pathogens ω respectively

Figure 19a shows that when the natural death rate of pathogens increases the carcasses decreases and pathogens also decreases.

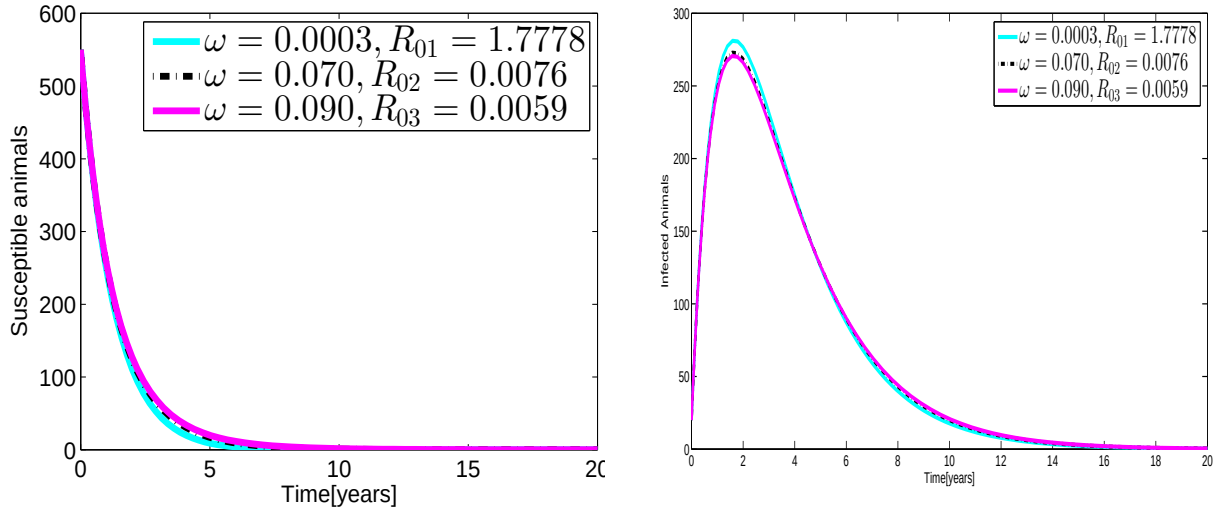

(a) Anthrax dynamics in susceptible animals **(b)** Anthrax dynamics in infected animals

Figure 20: Effect of pathogen's natural death rate to the dynamics of both susceptible animals and infected animals ω respectively

Figure 20 shows that when natural death rate of pathogen's increases susceptible animals increase while infected animals decrease. This is due to the fact that, the death of pathogens lower the anthrax infection. The study proposes fumigation, removal and burring/burning of carcasses, vaccination, and treatment to eradicate the disease. The effect of suggested controls

is discussed in the next section.

4.3.2 Numerical Simulation for Model with Anthrax Control Strategies

To determine how anthrax can be eradicated, control strategies such as fumigation, incineration, and removal of carcasses are proposed.

When pathogens are killed by fumigation, susceptible human and animals increase while infected human and animals decrease as shown in Figu. 21 and 22; respectively.

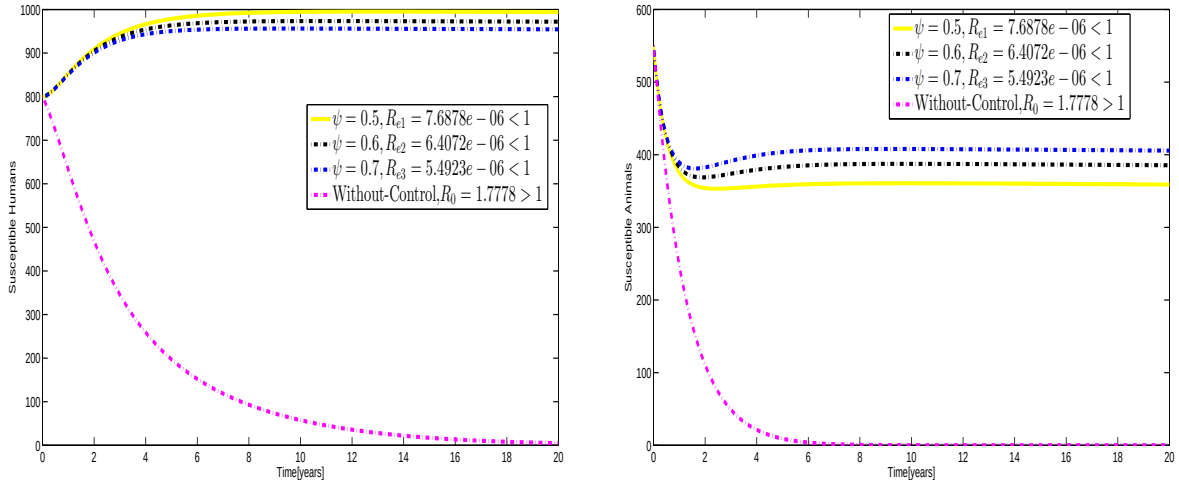

(a) Impact of fumigation to susceptible humans **(b)** Impact of fumigation to susceptible animals

Figure 21: Effect of fumigation to both susceptible humans and animals

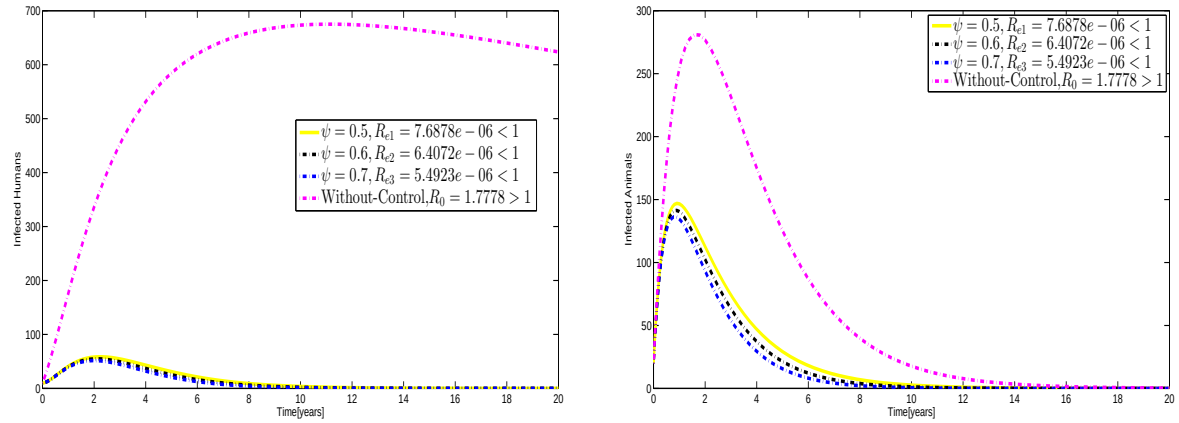

(a) Impact of fumigation to infected humans **(b)** Impact of fumigation to infected animals

Figure 22: Impact of destroying pathogens by use of fumigants to both infected animals and humans

In Fig. 22, the result shows that when fumigants such as formaldehyde, hydrogen peroxide are applied to the areas affected by free pathogens, both infected animals and humans decrease.

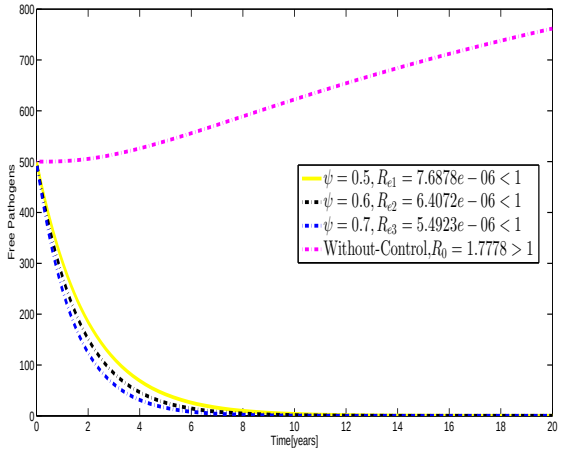

(a) Effect of fumigation on the pathogens population

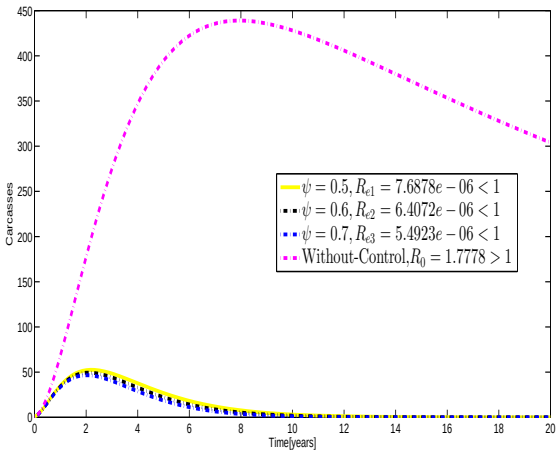

(b) Effect of fumigation to carcasses population

Figure 23: Effect of fumigants to carcasses and free pathogens population

In the Fig. 23, the result shows that when the rate of applying fumigants increase both pathogens and carcasses decrease.

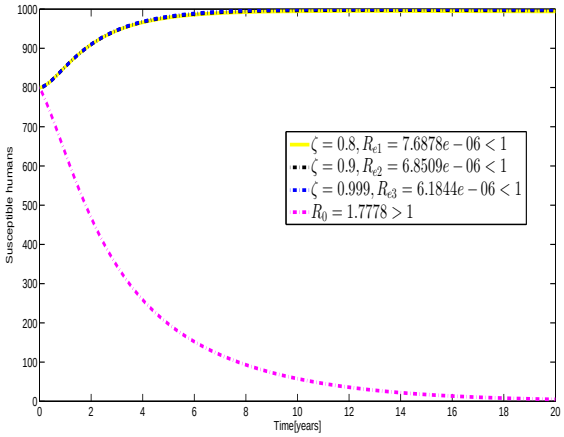

(a) Effect of incinerating and removal of carcasses to susceptible humans

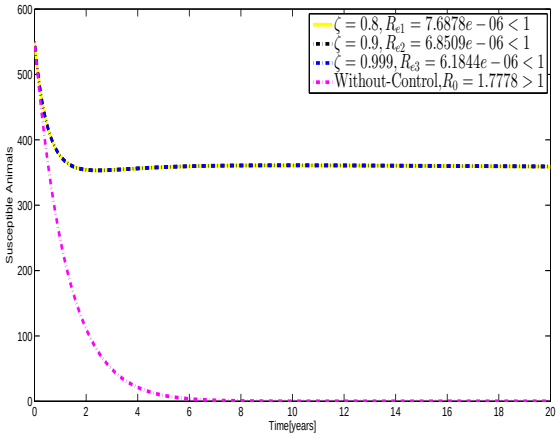

(b) Effect of incinerating and removal of carcasses to susceptible animals

Figure 24: Effect of incinerating and removal of carcasses to both susceptible animals and humans

In Fig. 24, the results depict that when the rate of completely removing and completely burning of carcasses in affected areas, susceptible humans and susceptible animals increase.

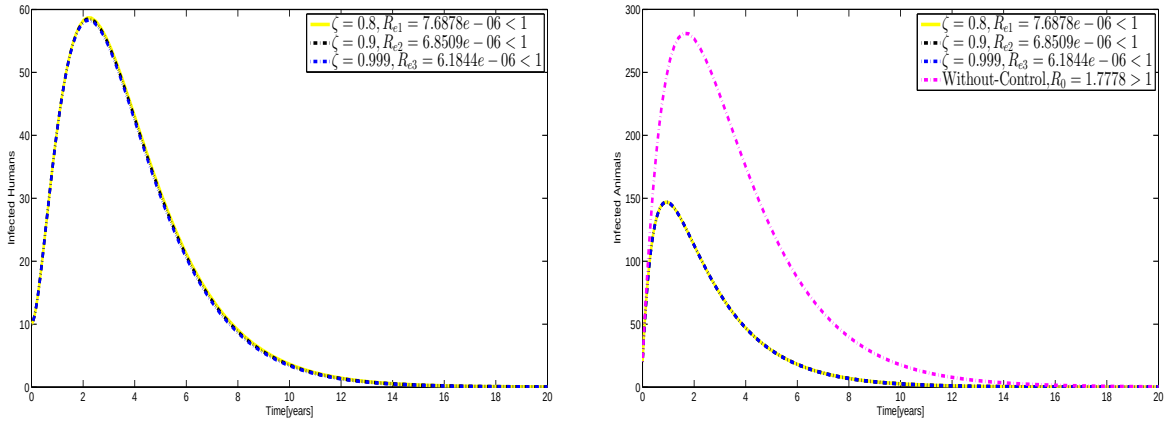

(a) Effect of incinerating and removal of carcasses to infected humans

(b) Effect of incinerating and removal of carcasses to infected animals

Figure 25: Effect of incinerating and removal of carcasses to both infected animals and humans

In Fig. 25, the results depict that when the rate of completely removing and completely burning of carcasses in affected areas increases, infected animals and humans decrease.

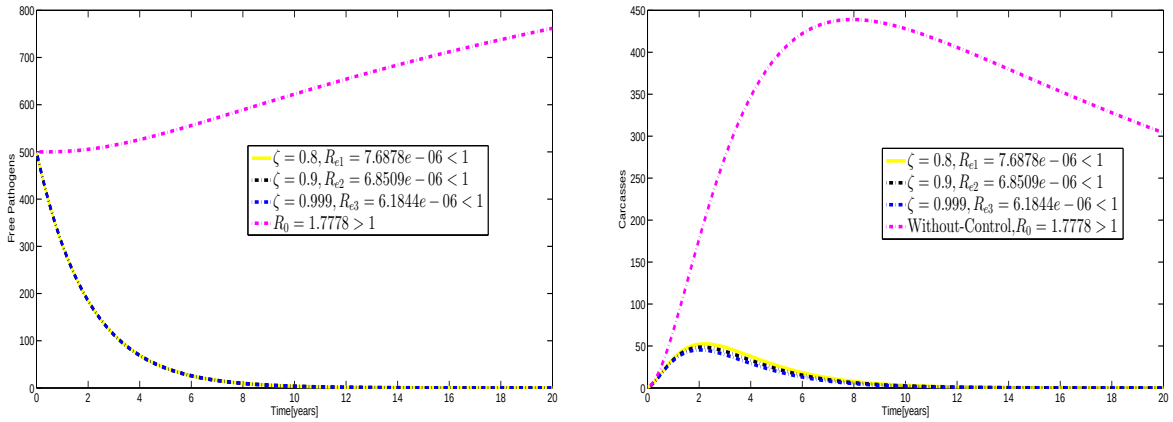

(a) Effect of incinerating and removal of carcasses to free pathogens

(b) Effect of incinerating and removal of carcasses to carcasses population

Figure 26: Effect of incinerating and removal of carcasses to both free pathogens and carcasses population

In Fig. 26, the results depict that when the rate of completely removing and completely burning of carcasses in affected areas increases, both free pathogens and carcasses decrease.

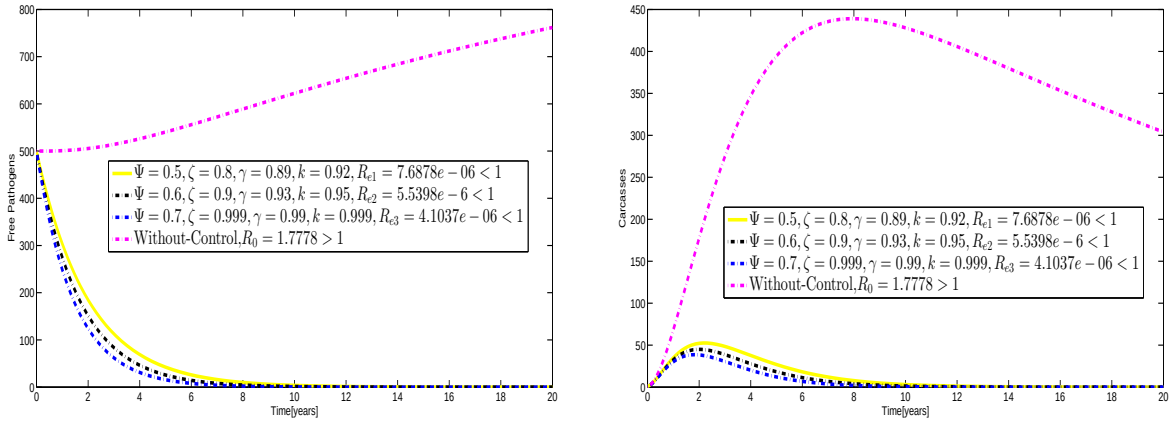

(a) Effect of all control strategies to free pathogens population

(b) Effect of all control strategies to carcasses population

Figure 27: Effect of incinerating and removal of carcasses, fumigation, animal's treatment and humane treatment to both free pathogens and carcasses population

In Fig. 27, the results depict that when the rate of completely removing and completely burning of carcasses, fumigation, animal's treatment and humane treatment in affected areas increases, both free pathogens and carcasses decrease.

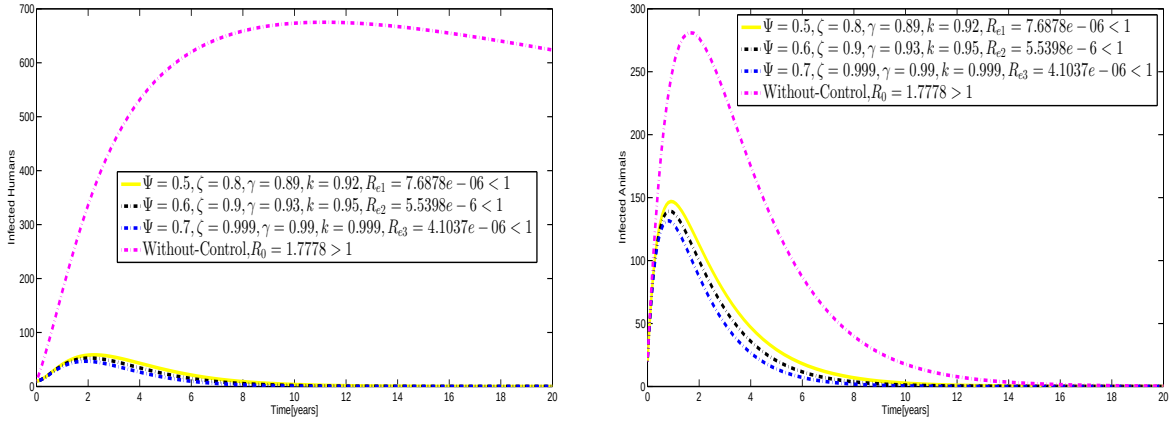

(a) Effect of all control strategies to infected humans population

(b) Effect of all control strategies to infected animals population

Figure 28: Effect of incinerating and removal of carcasses, fumigation, animal's treatment and humane treatment to both infected animals and humans

In Fig. 28, the results depict that when the rate of completely removing and completely burning of carcasses, fumigation, animal's treatment and humane treatment in affected areas increases, infected animals and humans decrease.

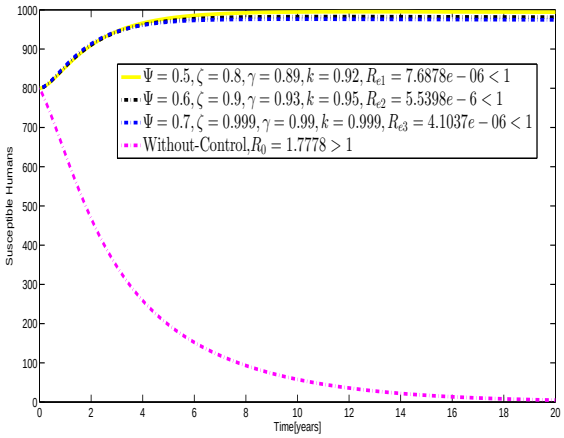

(a) Effect of incinerating and removal of carcasses, to susceptible humans

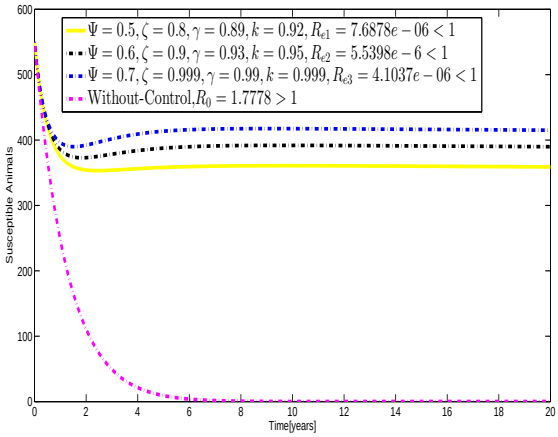

(b) Effect of incinerating and removal of carcasses, fumigation,animal's treatment and humans treatment to susceptible animals population

Figure 29: Effect of incinerating and removal of carcasses, fumigation, animal's treatment and humane treatment of both susceptible animals and humans population

In Fig. 29, the results depict that when the rate of completely removing and completely burning of carcasses, fumigation, animal's treatment and humane treatment in affected areas, susceptible humans and susceptible animals increase.

CHAPTER FIVE

CONCLUSION AND RECOMMENDATIONS

5.1 Conclusion

In this study mathematical models that describe the transmission dynamics of anthrax with and without control is developed and analyzed. The life cycle of anthrax in the two population is considered whereby the second model includes anthrax controls strategies. The basic reproduction number R_0 for the basic model is greater than unity showing that in the absence of control strategies anthrax will persist. Sensitivity analysis shows that; anthrax infection, animal death rate, animal recruitment rate and pathogen's death rate are more sensitive parameters to transmission dynamics of anthrax. Numerical simulation shows that infected humans, infected animals, pathogens and carcasses increase in proportion to animal infection rate. Susceptible humans and animals decrease as animal infection rate increases. Results further show that when the death rate of pathogens which are responsible for anthrax transmission increases, susceptible human and animals increase correspondingly while carcasses, infected humans and animals decrease consequently. To control anthrax infection, control strategies fumigation, incinerator, removal of carcasses and treatment are proposed. The analysis shows that control strategies are effective if in their implementation the effective reproduction R_e becomes less than one. Numerical analysis shows that when we increase fumigation rate, incinerating, removal of carcasses and treatment one at a time, susceptible human and animals increase while infected humans and animals, carcasses and pathogen decrease dramatically. This also occurs when all strategies are implemented concurrently. The anthrax infection rate, animal death rate, animal recruitment rate and pathogen's death rate are the most sensitive parameters to the basic reproduction. The descriptive statistics analysis shows that animals suffer mostly than humans which implies that animals get anthrax infection first followed by humans. The most sensitive parameters are variated by increasing and we find that they have a positive influence on the dynamics of anthrax. The controls strategies such as the use of fumigants, incineration of carcasses and earlier treatment of infected animals have the devastating effect towards anthrax transmission in both humans and animals population. Therefore, animal health centers are encouraged to educate its people about the stated controls measures. Animal's vaccination and environmental factors such as rainy and dry season are encouraged to be considered on the transmission and controls of anthrax for the future work of this study.

5.2 Recommendations

The study reveal that, anthrax transmission rate, animal death rate and animal's recruitment rate are the most sensitive parameters to the disease transmission thus the study recommends that, animals should be vaccinated and the affected environment should be fumigated. Also, we recommend the earlier treatment to both humans and animals. We also recommend that, stochastic differential equations should be considered in disease modeling since they are able to capture the real world situation.

This study recommends that the animal health centers under the use of their extension or field officers should encourage and educate their respective working communities on the preventive measures such as vaccination of animals, the use of protective gears for slaughterhouse workers. It also recommends that areas affected by anthrax should be well fumigated by the proper fumigants and carcasses should be incinerated and lastly, earlier treatment is encouraged to both humans and animals during the first signs stage of the disease.

As a way forward, this study has not exhausted everything as other studies too. To improve the findings of this work, an extension of the work on the inclusion of seasonality factors and parameters such as precipitation and temperature, valuable and constructive assumptions and other parameters that favor the growth and germination of anthrax pathogens is recommended. Also, the future work should use a Markov Chain Monte Carlo (MCMC) method for better parameter estimation and model fitting.

REFERENCES

Castillo-Chavez, C. (2002). Mathematical approaches for emerging and reemerging infectious diseases: an introduction. Vol. 1. Springer Science & Business Media.

Day, J., Friedman, A. and Schlesinger, L. S. (2011). Modeling the host response to inhalation anthrax. *Journal of Theoretical Biology*. **276**(1): 199–208.

Diekmann, O., Heesterbeek, J. A. P. and Metz, J. A. (1990). On the definition and the computation of the basic reproduction ratio in models for infectious diseases in heterogeneous populations. *Journal of Mathematical Biology*. **28**(4): 365–382.

for Animal Health, W. O. (2008). Anthrax in humans and animals. World Health Organization.

Friedman, A. and Yakubu, A. A. (2013). Anthrax epizootic and migration: persistence or extinction. *Mathematical Biosciences*. **241**(1): 137–144.

Furniss, P. and Hahn, B. (1981). A mathematical model of an anthrax epizoötic in the kruger national park. *Applied Mathematical Modelling*. **5**(3): 130–136.

Guckenheimer, J., Myers, M. and Sturmfels, B. (1997). Computing hopf bifurcations. *SIAM Journal on Numerical Analysis*. **34**(1): 1–21.

Hahn, B. D. and Furniss, P. R. (1983). A deterministic model of an anthrax epizootic: threshold results. *Ecological Modelling*. **20**(2-3): 233–241.

Hamby, D. (1994). A review of techniques for parameter sensitivity analysis of environmental models. *Environmental Monitoring and Assessment*. **32**(2): 135–154.

Harrington, R., Owen-Smith, N., Viljoen, P. C., Biggs, H. C., Mason, D. R. and Funston, P. (1999). Establishing the causes of the roan antelope decline in the kruger national park, south africa. *Biological Conservation*. **90**(1): 69–78.

Irunde, J. I., Luboobi, L. S. and Nkansah-Gyekye, Y. (2016). Modeling the effect of tobacco smoking on the in-host dynamics of HIV/AIDS. *Journal of Mathematical and Computational Science*. **6**(3): 406.

Korobeinikov, A. (2007). Global properties of infectious disease models with nonlinear incidence. *Bulletin of Mathematical Biology*. **69**(6): 1871–1886.

Korobeinikov, A. and Maini, P. K. (2004). A lyapunov function and global properties for sir and seir epidemiological models with nonlinear incidence. *Mathematical Biosciences and Engineering*. **1**(1): 57–60.

LaSalle, J. P. (1976). Stability theory and invariance principles. *In:* Dynamical Systems, Volume 1. Elsevier. pp. 211–222.

Lembo, T., Hampson, K., Auty, H., Beesley, C. A., Bessell, P., Packer, C., Halliday, J., Fyumagwa, R., Hoare, R. and Ernest, E. (2011). Serologic surveillance of anthrax in the serengeti ecosystem. *Emerging Infectious Diseases*. **17**(3): 387.

Mourez, M., Lacy, D. B., Cunningham, K., Legmann, R., Sellman, B. R., Mogridge, J. and Collier, R. J. (2002). 2001: a year of major advances in anthrax toxin research. *TRENDS in Microbiology*. **10**(6): 287–293.

Mushayabasa, S., Marijani, T. and Masocha, M. (2015). Dynamical analysis and control strategies in modeling anthrax. *Computational and Applied Mathematics*. pp. 1–16.

Mwakapeje, E. R., Høgset, S., Fyumagwa, R., Nonga, H. E., Mdegela, R. H. and Skjerve, E. (2018). Anthrax outbreaks in the humans-livestock and wildlife interface areas of northern tanzania: a retrospective record review 2006–2016. *BMC Public Health*. **18**(1): 106.

Myung, I. J. (2003). Tutorial on maximum likelihood estimation. *Journal of Mathematical Psychology*. **47**(1): 90–100.

Osman, S., Makinde, O. D. and Theuri, D. M. (2018). Mathematical modelling of transmission dynamics of anthrax in human and animal population. *Mathematical Theory and Modelling*. .

Raymond, B., Wyres, K. L., Sheppard, S. K., Ellis, R. J. and Bonsall, M. B. (2010). Environmental factors determining the epidemiology and population genetic structure of the bacillus cereus group in the field. *PLoS Pathogens*. **6**(5): e1000905.

Romero-Campero, F. J., Cao, H., Camara, M. and Krasnogor, N. (2008). Structure and parameter estimation for cell systems biology models. In: *Proceedings of the 10th Annual Conference on Genetic and Evolutionary Computation*. ACM. pp. 331–338.

Saad-Roy, C., van den Driessche, P. and Yakubu, A. A. (2017). A mathematical model of anthrax transmission in animal populations.. *Bulletin of Mathematical Biology*. **79**(2): 303–324.

Sinkie and Murthy, S. (2016). Modeling and simulation study of anthrax attack on environment. *Differential Equations*. **1**: 2.

Turnbull, P. (2002). Introduction: anthrax history, disease and ecology. *In:* Anthrax. Springer. pp. 1–19.

Ugwa, K. A. and Agwu, I. (2013). Mathematical analysis of the endemic equilibrium of thetransmission dynamics of tuberculosis.. *International Journal of Scientific and Technology Research*. **2**(12): 263–269.

Van den Driessche, P. and Watmough, J. (2002). Reproduction numbers and sub-threshold endemic equilibria for compartmental models of disease transmission. *Mathematical Biosciences*. **180**(1-2): 29–48.

APPENDICES

Appendix: MATLAB Codes

MATLAB codes for Chapter Three A.1 MATLAB codes for Figure 3.2

```
%Defining a function 'Ma.m' and its corresponding equations as follows:
function dy=Ma(~,y)
dy=zeros(size(y));
%parameter declaration
mua=0.0006;beta=0.0016;ba=0.0002;omega=0.0003;theta=0.0386;
pi=0.4141;mu_h=0.0002;b_h=0.0005;delta=0.0001;sigma=0.0005;phi=0.0003;
r = 0.0154;
%variable declaration
Sh=y(1);Ih=y(2);P=y(3);Sa=y(4);Ia=y(5);C=y(6);
%Equation of the model
dy(1)=b_h -(mu_h+sigma*Ia+delta*C+phi*P)*Sh;
dy(2)=(sigma*Ia+delta*C+phi*P)*Sh - (mu_h+r)*Ih;
dy(3)=theta*C-omega*P;
dy(4)=ba-beta*P*Sa-mua*Sa;
dy(5)=beta*P*Sa - (mua+pi)*Ia;
dy(6)=pi*Ia-theta*C;
%%%%%%%%%%%%%%%%%%%%%%%%%%
% RUNNING FILE;
clear all
clc
tspan =[2004 2016] ; %Time i n days ,
y0=[800, 10, 500, 550, 20,1];
[t,y]=ode45(@Ma,tspan,y0);
%MATHEMATICAL MODEL SIMULATION
figure(1)
set(gca,'FontSize',15)
set(legend,'FontSize',15)
plot(t,y(:,1),'b',t,y(:,2),'k',t,y(:,3),'r',t,y(:,4),'g',t,y(:,5),'y',...
t,y(:,6),'c','LineWidth',3.5);
legend('S_h=Susceptible humans','I_h=Infected humans','Free Pathoges','S_a=Susceptible animals','I_a=Infected animals','C=Carcass','Interpreter','Latex','FontSize',25);
xlabel('Time[years]');
ylabel('Populations');
title('Mathematical Model Simulations');
```

A.2 R codes for Figure 4.1 and 4.2

```
%\begin{verbatim}
x <- c(2005, 2006, 2007, 2008, 2009 ,2010 ,2011, 2012, 2013,
    2014, 2015, 2016)%Time[Years]
y1=c(8,32,48,12,11,15,22,21,37,58,42,18)%%Humans Infection
    cases
y2=c(28,50,67,30,22,38,36,27,46,78,67,22%%Animal infection
    cases
data <- data.frame(x, y1, y2)%% Data Frame
library(plotly)%% A command that invoke plotly package
p <- plot_ly(data, x = ~x, y = ~y1, type = 'bar', name = 'Human
     Cases', marker = list(color = 'rgb(49,130,189)')) %>%
+ add_trace(y = ~y2, name = 'Animal Cases', marker = list(color
    = 'rgb(204,204,204)')) %>%
+ layout(xaxis = list(title = , tickangle = -45),
+ yaxis = list(title = ),
+ margin = list(b = 100),
+ barmode = 'group')
*****++++++++++++**********++++++++++++++++++++++++++++++++
df1 <- data.frame(Time_years=Time_years,Anthrax_cases=y1,type=
    Animal
    Cases)
df2 <- data.frame(Time_years=Time_years,Anthrax_cases=y2,type=
    Human
    Cases)
df <- rbind(df1,df2)
ggplot(df)+geom_line(aes(Time_years,Anthrax_cases,colour=type,
    size=1.5))
```

A.3 MATLAB codes for Figure 4.3

```
function  dy=validatuly(t,y,theta)%%Function definition
dy=zeros(size(y));
%%Variable declaration
Sh=y(1);
Ih=y(2);
P=y(3);
Sa=y(4);
Ia=y(5);
C=y(6);
%%%%%Parameters to be estimated
beta=theta(1);
mua=theta(2);
ba=theta(3);
omega=theta(4);
theta1=theta(5);
mu_h=theta(6);
```

```
r=theta(7);
phi=theta(8);
b_h=theta(9);
delta=theta(10);
sigma=theta(11);
pi=theta(12);
%++++++++++++++++++++++++++++++++++++++++++++
dy(1)=b_h -(mu_h+sigma*Ia+delta*C+phi*P)*Sh;
dy(2)=(sigma*Ia+delta*C+phi*P)*Sh - (mu_h+r)*Ih;
dy(3)=theta1*C-omega*P;
dy(4)=ba-beta*P*Sa-mua*Sa;
dy(5)=beta*P*Sa - (mua+pi)*Ia;
dy(6)=pi*Ia-theta1*C;
%%%%%%%%%%%%%%%%%%%%%%%%%%%%%%%%%%%%%%%%%%%%
function E=ssfunvt(theta,data) % Objective funct. to be
    optimized for parameter estimation.
y=data.ydata; %
time=data.tdata;
y0=data.y0data;
[t, y_est]=ode45(@validatuly,time,y0,[],theta);
est_data = y_est(:,5);
E=sum(sum((y-est_data').^2));
%%++++++++++++++++++++++++++++++++++++
% RUNNING FILE;
clc
clear all; close all;
theta=[0.0001 0.0001 0.00001369 0.000014 0.001125 0.000045662
    0.00057  0.00001219 0.0015 0.0002 0.000125 0.06];%%Model
    Parameters declaration
y0=[70 10 50 55  10 1];%%Initial value condition for
    susceptible population
y=[8 32 48 12 11 15 22 21 37 58 42 18]; %first data for humans
    anthrax cases
y=[28 50 67 30 22 38 36 27 46 78 67 22];%%Animals anthrax cases
time = linspace(2004, 2016, length(y));
data.ydata=y;
data.tdata=time;
data.y0data=y0;
theta0=0.99*theta;
estimate=fminsearch(@ssfunvt,theta0,[],data);
tt = linspace(2004, 2016, 13);
[t,x]=ode45(@validatuly,tt,y0,[],estimate);
set(gca,'FontSize',14)
set(legend,'FontSize',14)
plot(time,y,'o-','LineWidth',6) % true data
hold on
```

```
x_est = x(:,5);
set(gca,'FontSize',14)
set(legend,'FontSize',14)
plot(t,x_est,'c-','LineWidth',6)
legend('True data','Fitted')
xlabel('Years')
ylabel('Infected Animals')
legend('True data','Fitted-Model-Output')
```

A.4 MATLAB codes for Figure 4.4, 4.5, 4.6,

```
%Defining a functions 'prev_inc_func1.m, prev_inc_func2.m,
    prev_inc_func1.m' and their corresponding equations as
    follows:
function dy=prev_inc_func1(~,y)
dy=zeros(size(y));
%parameter declaration
mua=0.0006;beta=0.0016;ba=0.0002;omega=0.0003;theta=0.0386;
pi=0.4141;mu_h=0.0002;b_h=0.0005;delta=0.0001;sigma=0.0005;phi
    =0.0003;
r = 0.0154;
%variable declaration
Sh=y(1);Ih=y(2);P=y(3);Sa=y(4);Ia=y(5);C=y(6);
%Equation of the model
dy(1)=b_h -(mu_h+sigma*Ia+delta*C+phi*P)*Sh;
dy(2)=(sigma*Ia+delta*C+phi*P)*Sh - (mu_h+r)*Ih;
dy(3)=theta*C-omega*P;
dy(4)=ba-beta*P*Sa-mua*Sa;
dy(5)=beta*P*Sa - (mua+pi)*Ia;
dy(6)=pi*Ia-theta*C;
R_01=beta.*ba.*(pi+mua)./((pi+mua).*omega.*mua)
**********++++++++++++++++++++++%%%
function dy=prev_inc_func2(~,y)
dy=zeros(size(y));
%parameter declaration
mua=0.0006;beta=0.0020;ba=0.0002;omega=0.0003;theta=0.0386;
pi=0.4141;mu_h=0.0002;b_h=0.0005;delta=0.0001;sigma=0.0005;phi
    =0.0003;
r = 0.0154;%variable declaration
Sh=y(1);Ih=y(2);P=y(3);Sa=y(4);Ia=y(5);C=y(6);
%Equation of the model
dy(1)=b_h -(mu_h+sigma*Ia+delta*C+phi*P)*Sh;
dy(2)=(sigma*Ia+delta*C+phi*P)*Sh - (mu_h+r)*Ih;
dy(3)=theta*C-omega*P;
dy(4)=ba-beta*P*Sa-mua*Sa;
dy(5)=beta*P*Sa - (mua+pi)*Ia;
```

```
dy(6)=pi*Ia-theta*C;
R_02=beta.*ba.*(pi+mua)./((pi+mua).*omega.*mua)
++++++++++++++++++++++++++++++++++++++++++++++++++++++++++++++++++++++++++++
function dy=prev_inc_func3(~,y)
dy=zeros(size(y));
%parameter declaration
mua=0.0006;beta=0.0030;ba=0.0002;omega=0.0003;theta=0.0386;
pi=0.4141;mu_h=0.0002;b_h=0.0005;delta=0.0001;sigma=0.0005;phi
    =0.0003;
r = 0.0154;
%variable declaration
Sh=y(1);Ih=y(2);P=y(3);Sa=y(4);Ia=y(5);C=y(6);
%Equation of the model
dy(1)=b_h -(mu_h+sigma*Ia+delta*C+phi*P)*Sh;
dy(2)=(sigma*Ia+delta*C+phi*P)*Sh - (mu_h+r)*Ih;
dy(3)=theta*C-omega*P;
dy(4)=ba-beta*P*Sa-mua*Sa;
dy(5)=beta*P*Sa - (mua+pi)*Ia;
dy(6)=pi*Ia-theta*C;
R_03=beta.*ba.*(pi+mua)./((pi+mua).*omega.*mua)
% RUNNING FILES;
clc
tspan =[0 20] ; %Time i n days ,
y0=[800 10 500 550 20 1];
[t1,y1]=ode45(@prev_inc_func1,tspan,y0);
[t2,y2]=ode45(@prev_inc_func2,tspan,y0);
[t3,y3]=ode45(@prev_inc_func3,tspan,y0);
%%%%%%%ANIMAL CASES
figure(1)
subplot(1,2,1)
set(gca,'FontSize',14)
set(legend,'FontSize',12)
plot(t1,y1(:,4),'c',t2,y2(:,4),'-.k',t3,y3(:,4),'m','LineWidth'
    ,4)
legend({'$\beta=0.0016,R_{01}=1.7778$','$\beta=0.0020,R_{02}=
    2.2222 $','$\beta=0.0030,R_{03}=3.3333$'},'Interpreter','
    Latex','FontSize',22)
xlabel('Time[years]')
ylabel('Susceptible animals')
hold on
subplot(1,2,2)
set(gca,'FontSize',15)
set(legend,'FontSize',15)
plot(t1,y1(:,5),'c',t2,y2(:,5),'-.k',t3,y3(:,5),'m','LineWidth'
    ,4)
legend({'$\beta=0.0016,R_{01}=1.7778$','$\beta=0.0020,R_{02}=
```

```
2.2222 $','$\beta=0.0030,R_{03}=3.3333$'},'Interpreter','Latex','FontSize',25)
xlabel('Time[years]')
ylabel('Infected Animals')
++++++++++++++++++++++++++++++++++++++++++++++++++++++++++++++++++++++++++++++++++++++
%%%%%FREE PATHOGENS AND CARCASSES
figure(2)
subplot(1,2,1)
set(gca,'FontSize',14)
set(legend,'FontSize',14)
plot(t1,y1(:,6),'g',t2,y2(:,6),'-k',t3,y3(:,6),'m','LineWidth',4)
legend({'$\beta=0.0016,R_{01}=1.7778$','$\beta=0.0020,R_{02}=2.2222 $','$\beta=0.0030,R_{03}=3.3333$'},'Interpreter','Latex','FontSize',20)
xlabel('Time[years]')
ylabel('Carcasses')
% grid on
subplot(1,2,2)
set(gca,'FontSize',14)
set(legend,'FontSize',12)
plot(t1,y1(:,3),'g',t2,y2(:,3),'-k',t3,y3(:,3),'m','LineWidth',4)
legend({'$\beta=0.0016,R_{01}=1.7778$','$\beta=0.0020,R_{02}=2.2222 $','$\beta=0.0030,R_{03}=3.3333$'},'Interpreter','Latex','FontSize',20)
xlabel('Time[years]')
ylabel('Pathogens')
********************HUMANS CASES
figure(3)
subplot(1,2,1)
set(gca,'FontSize',14)
set(legend,'FontSize',12)
plot(t1,y1(:,1),'-.b',t2,y2(:,1),'r',t3,y3(:,1),'-.k','LineWidth',2.5)
legend({'$\beta=0.0016,R_{01}=1.7778$','$\beta=0.0020,R_{02}=2.2222 $','$\beta=0.0030,R_{03}=3.3333$'},'Interpreter','Latex','FontSize',20)
xlabel('Time[years]')
ylabel('Susceptible humans')
hold on
subplot(1,2,2)
set(gca,'FontSize',14)
set(legend,'FontSize',12)
plot(t1,y1(:,2),'-.b',t2,y2(:,2),'r',t3,y3(:,2),'-.k','
```

```
    LineWidth',2.5)
107 legend({'$\beta=0.0016,R_{01}=1.7778$','$\beta=0.0020,R_{02}=
    2.2222 $','$\beta=0.0030,R_{03}=3.3333$'},'Interpreter','
    Latex','FontSize',20)
108 xlabel('Time[years]')
109 ylabel('Infected humans')
```

A.4 MATLAB codes for Figure 4.19, 4.20, 4.21

```
1  %Defining a functions 'Function1.m,Function2.m,Function3.m' and
       their corresponding equations as follows:
2  function dy=Function1(~,y)
3  dy=zeros(size(y));
4  %parameter declaration
5  mua=0.0006;beta=0.0016;ba=0.0002;omega=0.0003;alpha=0.0186;
6  pi=0.4141;mu_h=.0002;b_h=0.0005;delta=0.0001;sigma=0.0005;phi
       =0.00001219;
7  r = 0.000547;%alpha=0.01;
8  gamma=0.89;psi=0.5;k=0.92;zeta=0.8;
9  %variable declaration
10 Sh=y(1);Ih=y(2);P=y(3);Sa=y(4);Ia=y(5);C=y(6);
11 %Equation of the model
12 dy(1)=b_h+k*Ia -(mu_h+sigma*Ia+delta*C+phi*P)*Sh;
13 dy(2)=(sigma*Ia+delta*C+phi*P)*Sh - (mu_h+r+k)*Ih;
14 dy(3)=alpha*C-(omega+psi)*P;
15 dy(4)=ba+gamma*Ia-beta*P*Sa-mua*Sa;
16 dy(5)=beta*P*Sa - (mua+pi+gamma)*Ia;
17 dy(6)=pi*Ia-(alpha+zeta)*C;
18 Re1=beta*ba*alpha*pi./(mua.*(gamma+pi+mua).*(alpha+zeta).*(
       omega+psi))
19 ++++++++++++++++++++++++++++++++++++++++++++++++++++++++++
20 function dy=Function2(~,y)
21 dy=zeros(size(y));
22 %parameter declaration
23 mua=0.0006;beta=0.0016;ba=0.0002;omega=0.0003;alpha=0.0186;
24 pi=0.4141;mu_h=.0002;b_h=0.0005;delta=0.0001;sigma=0.0005;phi
       =0.00001219;
25 r = 0.000547;%alpha=0.01;
26 gamma=0.93;psi=0.6;k=0.95;zeta=0.9;
27 %variable declaration
28 Sh=y(1);Ih=y(2);P=y(3);Sa=y(4);Ia=y(5);C=y(6);
29 %Equation of the model
30 dy(1)=b_h+k*Ia -(mu_h+sigma*Ia+delta*C+phi*P)*Sh;
31 dy(2)=(sigma*Ia+delta*C+phi*P)*Sh - (mu_h+r+k)*Ih;
32 dy(3)=alpha*C-(omega+psi)*P;
```

```
dy(4)=ba+gamma*Ia-beta*P*Sa-mua*Sa;
dy(5)=beta*P*Sa - (mua+pi+gamma)*Ia;
dy(6)=pi*Ia-(alpha+zeta)*C;
Re2=beta*ba*alpha*pi./(mua.*(gamma+pi+mua).*(alpha+zeta).*(omega+psi))
% &&&&&&&&&&&&&&&&&&&&&&&&&&&&&&&&&&&&&&&&&&&&&&&&&&&&&&&&&&&&&&&+++++++++

function dy=Function3(~,y)
dy=zeros(size(y));
%parameter declaration
mua=0.0006;beta=0.0016;ba=0.0002;omega=0.0003;alpha=0.0186;
pi=0.4141;mu_h=.0002;b_h=0.0005;delta=0.0001;sigma=0.0005;phi=0.00001219;
r = 0.000547;%alpha=0.01;
gamma=0.99;psi=0.7;k=0.999;zeta=0.999;
%variable declaration
Sh=y(1);Ih=y(2);P=y(3);Sa=y(4);Ia=y(5);C=y(6);
%Equation of the model
dy(1)=b_h+k*Ia -(mu_h+sigma*Ia+delta*C+phi*P)*Sh;
dy(2)=(sigma*Ia+delta*C+phi*P)*Sh - (mu_h+r+k)*Ih;
dy(3)=alpha*C-(omega+psi)*P;
dy(4)=ba+gamma*Ia-beta*P*Sa-mua*Sa;
dy(5)=beta*P*Sa - (mua+pi+gamma)*Ia;
dy(6)=pi*Ia-(alpha+zeta)*C;
Re3=beta*ba*alpha*pi./(mua.*(gamma+pi+mua).*(alpha+zeta).*(omega+psi))
+++++++++++++++++++++++++++++++++++++++++++++++++++
%%RUNNING FILES
clear all
clc
tspan =[0 20] ; %Time i n days ,
y0=[800 10 500 550 20 1];
% y0=[500, 0, 0, 5000, 700, 0];
%opt = odeset ('RelTol', 2.22045*exp(-14));%c r e a t e s an i n t e g r a t o r
[t1,y1]=ode45(@Function1,tspan,y0);
[t2,y2]=ode45(@Function2,tspan,y0);
[t3,y3]=ode45(@Function3,tspan,y0);
[t4,y4]=ode45(@prev_inc_func1 ,tspan,y0);
figure(1)
% subplot(1,2,1)
set(gca,'FontSize',14)
set(legend,'FontSize',12)
plot(t1,y1(:,1),'y',t2,y2(:,1),'-.k',t3,y3(:,1),'-.b',t4,y4(:,1),'-m','LineWidth',4)
```

```
72  legend({'$\Psi=0.5,\zeta=0.8,\gamma=0.89,k=0.92,R_{e1}=7.6878e
        -06 < 1$','$\Psi=0.6,\zeta=0.9,\gamma=0.93,k=0.95,R_{e2}=
        5.5398e-6 < 1 $','$\Psi=0.7,\zeta=0.999,\gamma=0.99,k=0.999,
        R_{e3}= 4.1037e-06 < 1 $','Without-Control,$R_{0}=1.7778 >
        1$'},'Interpreter','Latex','FontSize',22)
73  xlabel('Time[years]')
74  ylabel('Susceptible Humans')
75  figure(2)
76  % subplot(1,2,1)
77  set(gca,'FontSize',14)
78  set(legend,'FontSize',12)
79  plot(t1,y1(:,2),'y',t2,y2(:,2),'-.k',t3,y3(:,2),'-.b',t4,y4
        (:,2),'-.m','LineWidth',4)
80  legend({'$\Psi=0.5,\zeta=0.8,\gamma=0.89,k=0.92,R_{e1}=7.6878e
        -06 < 1$','$\Psi=0.6,\zeta=0.9,\gamma=0.93,k=0.95,R_{e2}=
        5.5398e-6 < 1 $','$\Psi=0.7,\zeta=0.999,\gamma=0.99,k=0.999,
        R_{e3}= 4.1037e-06 < 1 $','Without-Control,$R_{0}=1.7778 >
        1$'},'Interpreter','Latex','FontSize',22)
81  xlabel('Time[years]')
82  ylabel('Infected Humans')
83  figure(3)
84  % subplot(1,2,1)
85  set(gca,'FontSize',14)
86  set(legend,'FontSize',12)
87  plot(t1,y1(:,3),'y',t2,y2(:,3),'-.k',t3,y3(:,3),'-.b',t4,y4
        (:,3),'-.m','LineWidth',4)
88  legend({'$\Psi=0.5,\zeta=0.8,\gamma=0.89,k=0.92,R_{e1}=7.6878e
        -06 < 1$','$\Psi=0.6,\zeta=0.9,\gamma=0.93,k=0.95,R_{e2}=
        5.5398e-6 < 1 $','$\Psi=0.7,\zeta=0.999,\gamma=0.99,k=0.999,
        R_{e3}= 4.1037e-06 < 1 $','Without-Control,$R_{0}=1.7778 >
        1$'},'Interpreter','Latex','FontSize',22)
89  xlabel('Time[years]')
90  ylabel('Free Pathogens')
91  figure(4)
92  % subplot(1,2,1)
93  set(gca,'FontSize',14)
94  set(legend,'FontSize',12)
95  plot(t1,y1(:,4),'y',t2,y2(:,4),'-.k',t3,y3(:,4),'-.b',t4,y4
        (:,4),'-.m','LineWidth',4)
96  legend({'$\Psi=0.5,\zeta=0.8,\gamma=0.89,k=0.92,R_{e1}=7.6878e
        -06 < 1$','$\Psi=0.6,\zeta=0.9,\gamma=0.93,k=0.95,R_{e2}=
        5.5398e-6 < 1 $','$\Psi=0.7,\zeta=0.999,\gamma=0.99,k=0.999,
        R_{e3}= 4.1037e-06 < 1 $','Without-Control,$R_{0}=1.7778 >
        1$'},'Interpreter','Latex','FontSize',22)
97  xlabel('Time[years]')
98  ylabel('Susceptible Animals')
```

```
figure(5)
% subplot(1,2,1)
set(gca,'FontSize',14)
set(legend,'FontSize',12)
plot(t1,y1(:,5),'y',t2,y2(:,5),'-.k',t3,y3(:,5),'-.b',t4,y4
    (:,5),'-.m','LineWidth',4)
legend({'$\Psi=0.5,\zeta=0.8,\gamma=0.89,k=0.92,R_{e1}=7.6878e
    -06 < 1$','$\Psi=0.6,\zeta=0.9,\gamma=0.93,k=0.95,R_{e2}=
    5.5398e-6 < 1 $','$\Psi=0.7,\zeta=0.999,\gamma=0.99,k=0.999,
    R_{e3}= 4.1037e-06 < 1 $','Without-Control,$R_{0}=1.7778 >
    1$'},'Interpreter','Latex','FontSize',22)
xlabel('Time[years]')
ylabel('Infected Animals')
figure(6)
% subplot(1,2,1)
set(gca,'FontSize',14)
set(legend,'FontSize',12)
plot(t1,y1(:,6),'y',t2,y2(:,6),'-.k',t3,y3(:,6),'-.b',t4,y4
    (:,6),'-.m','LineWidth',4)
legend({'$\Psi=0.5,\zeta=0.8,\gamma=0.89,k=0.92,R_{e1}=7.6878e
    -06 < 1$','$\Psi=0.6,\zeta=0.9,\gamma=0.93,k=0.95,R_{e2}=
    5.5398e-6 < 1 $','$\Psi=0.7,\zeta=0.999,\gamma=0.99,k=0.999,
    R_{e3}= 4.1037e-06 < 1 $','Without-Control,$R_{0}=1.7778 >
    1$'},'Interpreter','Latex','FontSize',22)
xlabel('Time[years]')
ylabel('Carcasses')
```

Output1: Published Paper

Available online at http://scik.org
J. Math. Comput. Sci. 8 (2018), No. 6, 654-672
https://doi.org/10.28919/jmcs/3798
ISSN: 1927-5307

MODELING THE TRANSMISSION DYNAMICS OF ANTHRAX DISEASE IN CATTLE AND HUMANS

JOELY E EFRAIM[1,*], JACOB ISMAIL IRUNDE[2] , DMITRY KUZNETSOV[1]

[1]Department of Mathematics, The Nelson Mandela African Institution of Science and Technology, Arusha, Tanzania

[2]Department of Mathematics, Mkwawa University College of Education,Iringa, Tanzania

Abstract. Anthrax is a zoonotic disease caused by bacillus anthraces. In this study a deterministic mathematical model for transmission dynamics of anthrax in humans and animals is presented and quantitatively analyzed. To understand the dynamics of anthrax, the basic reproduction number R_0 which measures average new infections is computed using next generation matrix operator and analyzed by normalized forward sensitivity index. Analysis shows that anthrax transmission rate to animals, animals' natural death rate, anthrax natural death rate and animal's birth rate are the most sensitive parameters to the disease transmission dynamics. When animal recruitment and anthrax transmission rates increase, the basic reproduction number R_0 also increase proportionally. However, when animal natural and anthrax induced death rates increase, basic reproduction number R_0 decreases. Numerical simulations using Runge-Kutta method show that animals drive the dynamics of anthrax. The study suggests control strategies such as vaccination, fumigation and decomposition of carcasses to eradicate the disease.

Keywords: sensitivity analysis; zoonotic disease; mathematical model; humans; cattle.

2010 AMS Subject Classification: 00A71, 00A72, 92B05, 92D30 .

*Corresponding author

E-mail address: efraimj@nm-aist.ac.tz

Received July 12, 2018

1. Introduction

Anthrax is an acute infectious disease caused by bacterium Bacillus anthraces [10]. The disease is transmitted in four different forms that includes, inhalation, ingestion, contact and injection. Herbivorous are more vulnerable to infection when they eat spores in the soil or plants, [15]. Omnivorous as well are vulnerable to the disease and they catch the infection through eating meat which is contaminated with anthrax. There are four types of anthrax which are inhalation, ingestion or gastrointestinal, injection and cutaneous anthrax [12].

Grasses serve as exploited habitats of bacillus anthracis and grazing animals such as sheep, goat and cattle are predominantly victims [13]. The alkaline soil with a pH greater than 6.0, high nitrogen level caused by decaying vegetation in soil, balanced periods of rain, droughts and temperature higher than 15 degrees Celsius facilitate the occurrence of anthrax and influence the ecology and survival of the bacterium bacillus anthraces [9]. The life span of bacillus anthraces is approximated to be 200 years [10]. They die naturally and during rain season at a rate of 0.000014 day^{-1} [12].

Anthrax is a zoonotic disease which is transmitted from infected animal to human beings. Humans are vulnerable to cutaneous type of anthrax [14]. In the cycle of anthrax, the environment as the pathogen's reservoir serves as the central source of the infection. Cattle get the disease during grazing period especially in rain and dry season. An infected animal can cycle the spores or pathogens (bacillus anthraces) again back to the environment during excretion [12]. Humans catch the disease through contacting an infected animal's product during butchering and slaughtering and when eating raw meat from infected animal.

Anthrax has persisted in Africa where for example in Kruger National Park in South Africa, number of roan antelope declined from 450 to 45 animals [5]. In Tanzania, 109 black wildbeest, 21 grant's gazelle,10 cattles and 26 goats died, [8]. Also in Kilimanjaro region, three villages reported hospitalization of 36 who ate anthrax contaminate meat from a cow [11]. In Arusha as well it has been reported that out of 134 people infected with anthrax, 8 died. Also, in Dar es Salaam out of 22 infected people, 6 died [11].

To provide better understanding of anthrax dynamics and suggest control measures to eradicate the disease mathematical models are of paramount importance. Few mathematical models

have been developed. Keeling and Rohani [7] developed mathematical model for anthrax basing on environmental contamination and contact between uninfected animals and infected carcases. The analysis shows that environmental contamination determines the threshold value for the model.

Furniss and Hahn [3] formulated the mathematical model basing on environmental contamination and direct contact between infected animals and non-infected carcasses. The model exhibit the threshold value determined by an environmental contamination parameter. Friedman and Yakubu [2] used a mathematical model developed by Hahn and Furnish and study anthrax is transmitted through carcass ingestion, spread of carcasses to the environment and migration rates on the persistence of animal population. The analysis shows that the spread of carcasses to the environment increases the transmission of the disease. Though the problem is addressed, infection between animals and human being in the transmission dynamics of anthrax is not considered. By modifying the models developed by [14-10], this work is intending to study the dynamics of anthrax when infection between animals and human being is considered.

2. Materials and Methods

2.1 Model Development

The model for anthrax is formulated by extending the models which were developed by Mushayabasa [10] and Sinkie [14] to include human beings. Dynamics of anthrax divides human and animal population each into two classes: susceptible S_h and infected I_h humans, and susceptible S_a and infected I_a animals respectively. Carcasses' class is represented by C.

Susceptible humans increase due to birth at a rate b_h and decrease due to anthrax infection after eating meat from infected animal and carcasses at a rate σ. They also can acquire the disease when they eat or comes into contact with infected carcasses at a rate δ and when they come into contact with environment which is contaminated with pathogen at a rate ϕ. However, infected humans increase at a rate σ when susceptible human eat meat from infected animal and carcasses. Infected humans also increase when susceptible human eat or come into contact with infected carcasses at a rate δ and also when they come into contact with environment which is

contaminated with pathogens at a rate ϕ . However, infected humans decrease due to anthrax and natural induced death at rates r and μ_h respectively.

Susceptible animals replenish due to birth at a rate b_a, however, they decrease due to anthrax infection following contact with pathogens at a rate β. Infected animals increase following infection of susceptible animal at a rate β, they suffer disease induced death at a rate π. All animal classes suffer natural mortality at a rate μ_a.

Infected animals die due to anthrax and become carcasses at a rate π. The carcasses increase at rate of π due to anthrax induced death rate and decrease due to decomposition at a rate of θ and shed pathogens to the environment at a rate θ. The pathogens increase at a rate of θ following carcass's decomposition and decrease at a rate of ω due to natural death and sometimes due to rain flushing off. The interaction between infected animals, environment and humans is well illustrated by the Figure 1

2.2 Model assumptions

The model assumes that all animals and humans are susceptible to the disease. The recruitment rate for new individual is through birth. No incubation period for both animals and humans. Huamans and animals suffer natural mortality at rates μ_h and μ_a respectively. Infected animals and environment are the main source of infections. Carcasses shed pathogens to environment through excretion[12].

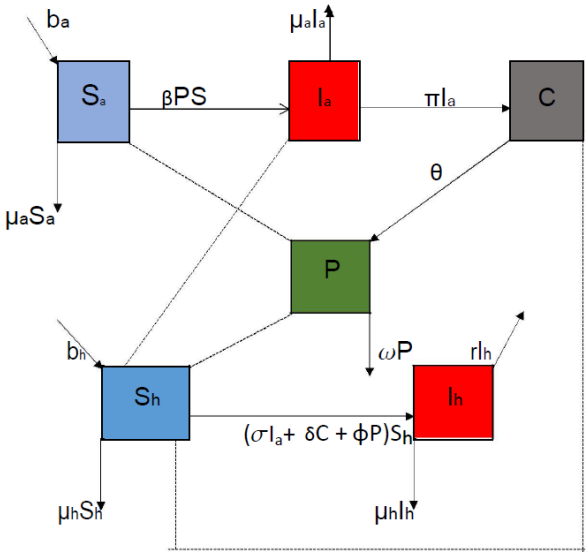

FIGURE 1. The model compartment-mental diagram

Placing together both formulation and assumptions, model which describes the interaction animals, humans and environment is given by:

$$\frac{dS_h}{dt} = b_h - (\sigma I_a + \delta C + \phi P + \mu_h)S_h \tag{1a}$$

$$\frac{dI_h}{dt} = (\sigma I_a + \delta C + \phi P)S_h - (\mu_h + r)I_h \tag{1b}$$

$$\frac{dP}{dt} = \theta C - \omega P \tag{1c}$$

$$\frac{dS_a}{dt} = b_a - (\beta P + \mu_a)S_a \tag{1d}$$

$$\frac{dI_a}{dt} = \beta P S_a - (\mu_a + \pi)I_a \tag{1e}$$

$$\frac{dC}{dt} = (\pi + \mu_a)I_a - \theta C \tag{1f}$$

$S_h(0) > 0; I_h(0) \geq 0; P(0) \geq 0; S_a(0) > 0; I_a(0) \geq 0; C(0) \geq 0$

2.3 Invariant region

Invariant region shows the boundedness of solutions. To determine the region, human, animal and pathogens' population are considered each separately. Humans, animal and pathogens' populations denoted by N_h, N_a and P respectively. Human population is given by:

$$N_h = S_h + I_h$$

$$\frac{dN_h}{dt} \leq b_h - \mu_h S_h \tag{2}$$

Solving the inequality (2) we get:

$$N_h(t) \leq \frac{b_h}{\mu_h} + \left(N_h(0) - \frac{b_h}{\mu_h}\right) e^{-\mu_h t} \tag{3}$$

but as t tends to infinity then: $N_h \leq \frac{b_h}{\mu_h}$ for $N_h(0) = S_h(0) + I_h(0)$.
For animal population:

$$N_a = S_a + I_a + C \tag{4}$$

$$\frac{dNa}{dt} \leq b_a - \mu_a N_a \tag{5}$$

Therefore the solution is given by:

$$N_a(t) \leq \frac{b_a}{\mu_a} + \left(N_a(0) - \frac{b_a}{\mu_a}\right) e^{-\mu_a t} \tag{6}$$

For $N_a(0) = S_a(0) + I_a(0) + C(0)$

Analysis of solution (6) considers two cases:

When $N_a(0) \geq \frac{b_a}{\mu_a}$ and $N_a(0) \leq \frac{b_a}{\mu_a}$. When $N_a(0) \geq \frac{b_a}{\mu_a}$

$$N_a(t) \leq \frac{b_a}{\mu_a} + \left(N_a(0) - \frac{b_a}{\mu_a}\right) e^{-\mu_a t}$$

Since:

$$\lim_{t\to\infty} \left(N_a(0) - \frac{b_a}{\mu_a}\right) e^{-\mu_a t} = \infty$$

then:

$$N_a(t) \leq \frac{b_a}{\mu_a}$$

From the definition of N_a, it follows that:

$$\lim_{t\to\infty} S_a \leq \frac{b_a}{\mu_a}, \lim_{t\to\infty} I_a \leq \frac{b_a}{\mu_a}, \lim_{t\to\infty} C \leq \frac{b_a}{\mu_a}$$

For pathogen population we have:

$$\frac{dP}{dt} = \theta C - \omega P, \ put\ C \leq \frac{b_a}{\mu_a}$$
$$\frac{dP}{dt} \leq \theta \frac{b_a}{\mu_a} - \omega P \tag{7}$$

Solving the inequality (7) we get:

$$P(t) = \theta \frac{b_a}{\omega \mu_a} + \left(P(0) - \theta \frac{b_a}{\omega \mu_a}\right) e^{\omega \mu_a t} \tag{8}$$

It follows that, analysis of the solution (8) considers two cases, these are: $P(0) > \frac{\theta b_a}{\omega \mu_a}$ and $P(0) < \frac{\theta b_a}{\omega \mu_a}$. When: $P(0) > \frac{\theta b_a}{\omega \mu_a}$
we have:

$$P(0) \leq \theta \frac{b_a}{\omega \mu_a} \leq \theta \frac{b_a}{\omega \mu_a} + \left(P(0) - \theta \frac{b_a}{\omega \mu_a} \right) e^{\omega t}$$

and when:

$$P(0) < \frac{\theta b_a}{\omega \mu_a}$$

, we have:

$$P(0) \leq \theta \frac{b_a}{\omega \mu_a} \leq \theta \frac{b_a}{\omega \mu_a} + \left(P(0) - \theta \frac{b_a}{\omega \mu_a} \right) e^{\omega t}$$

Since:

$$\left(P(0) - \theta \frac{b_a}{\omega \mu_a} \right) e^{-\omega t} \to 0$$

then:

$$\lim_{t \to \infty} P < \frac{b_a}{\omega \mu_a}$$

Therefore the model system (1) is positive invariant in the region:
$\Gamma = \{(S_a, I_a, C, P, S_h, I_h) \in R_+^6 : 0 \leq S_a + I_a + C \leq \frac{b_a}{\mu_a}, 0 \leq P \leq \theta \frac{b_a}{\omega \mu_a}, 0 \leq S_h + I_h \leq \frac{b_h}{\mu_h}\}$.
Solution for the model system (1) which begins on the boundary of the boundary region Γ converge to the region and remain bounded. Therefore the model (1) is mathematically and epidemiologically meaningful and we can consider flow generated for analysis. This result is summarized in the following theorem;

Theorem: Solutions of the model system (1) enter the region:
$\Gamma = \{(S_a, I_a, C, P, S_h, I_h) \in R_+^6 : 0 \leq S_a + I_a + C \leq \frac{b_a}{\mu_a}, 0 \leq P \leq \theta \frac{b_a}{\omega \mu_a}, 0 \leq S_h + I_h \leq \frac{b_h}{\mu_h}\}$

2.4 Positivity of solutions

Theorem: *Let the initial value of variables of the model* (1) *be* $S_a(0) > 0, I_a(0) > 0, P(0) > 0, C(0) > 0, S_h(0) > 0$ *and* $I_h(0) > 0$. *Then the solution set* $\Gamma = \{S_a(0) > 0, I_a(0) > 0, P(0) > 0, C(0) > 0, S_h(0) > 0, I_h(0) > 0\}$ *is positive for all time t.*

Proof: Lets consider the equation number (1a) of the model system (1), we have:

$$\begin{aligned} \frac{dS_a}{dt} &= b_a - (\beta P + \mu_a)S_a \\ \frac{dS_a}{dt} &\geq -(\beta P + \mu_a)S_a \end{aligned} \tag{9}$$

By separating variables we get:

$$\frac{dS_a}{S_a} \geq -(\beta P + \mu_a)dt \tag{10}$$

By integrating both sides, we get;

$$\begin{aligned} \int \frac{dS_a}{S_a} &\geq \int_0^t (\beta P + \mu_a)dt \\ \ln S_a &\geq -\int_0^t (\beta P + \mu_a)dt + C \\ S_a(t) &\geq e^{\int_0^t -(\beta P + \mu_a)t} \end{aligned} \tag{11}$$

At initial condition, we get;

$$\begin{aligned} S_a(t) &\geq S_a(0)e^{\int_0^t (\beta P(s) + \mu_a)dt} \\ S_a(t) &\geq S_a(0)e^{\int_0^t (\beta P(s) + \mu_a)dt} \end{aligned} \tag{12}$$

Then, $S_a(t) \geq 0, \forall\, t \geq 0$

From the equation number (1b) of the model (1) we have;

$$\begin{aligned} \frac{dI_a}{dt} &= \beta P S_a - (\mu_a + \pi)I_a \\ \frac{dI_a}{dt} &\geq -(\mu_a + \pi) \\ \frac{dI_a}{I_a} &\geq -(\mu_a + \pi)dt \\ \int \frac{dI_a}{I_a} &\geq -\int_0^t (\mu_a + \pi)dt \\ I_a(t) &\geq I_a(0)e^{-(\mu_a + \pi)t} \geq 0 \end{aligned} \tag{13}$$

From the equation (1c) of the model (1), we have;

$$\begin{aligned} \frac{dC}{dt} &= \pi I_a - \theta C \\ \frac{dC}{dt} &\geq -\theta C \\ \int \frac{dC}{C} &= -\int_0^t \theta dt \\ C(t) &\geq C(0)e^{-\theta t} \geq 0. \end{aligned} \tag{14}$$

From the equation number (1d) of the model (1), we have;

$$\begin{aligned} \frac{dP}{dt} &= \theta C - \omega P \\ \frac{dP}{dt} &\geq -\omega P \\ \frac{dP}{P} &= \int_0^t -\omega dt \end{aligned} \tag{15}$$

Solving (15) we get:

$$P(t) \geq P(0)e^{-\omega t} \geq 0$$

Again from the equation (1e) of the model (1), we have;

$$\begin{aligned} \frac{dS_h}{dt} &= b_h - (\sigma I_h + \delta C + \mu_h + \phi P)S_h \\ \int \frac{dS_h}{S_h} &\geq -\int_0^t (\sigma I_h + \delta C + \mu_h + \phi P)dt \\ S_h(t) &\geq S_h(0)e^{-\int_0^t (\sigma I_h + \delta C + \mu_h + \phi P)dt} \geq 0 \end{aligned} \tag{16}$$

From the equation number (1f) of the model (1), we have;

$$\begin{aligned} \frac{dI_h}{dt} &= (\sigma I_h + \delta C + \phi P)S_h - (\mu_h + r)I_h \\ \frac{dI_h}{dt} &\geq -(\mu_h + r)I_h \\ \int \frac{dI_h}{I_h} &= \int_0^t -(\mu_h + r)dt \end{aligned} \tag{17}$$

$$I_h t \geq I_h(0)e^{-(\mu_h + r)t} \geq 0$$

2.5 The basic reproduction number R_0

The basic reproduction number is the average number of secondary infections generated by a single individual when introduced in an entirely susceptible population [1, 6]. It determines whether the disease persists or clears out. The disease clears out when $R_0 < 1$ and persists when $R_0 > 1$ [6].

To compute basic reproduction number, we adopt the next generation matrix method where new infections and transfer terms are considered. If the new infections are mathematically defined by f_i and transfer terms by v_i, then the matrices F and V are given by

$$F = \frac{\partial f_i}{\partial X_j}(x_0) \text{ and } V = \frac{\partial v_i}{\partial X_j}(x_0) \tag{18}$$

as defined by Van den Driessche and Watmough [16] . The basic reproduction number R_0 is therefore given by:

$$R_0 = \rho(FV^{-1}). \tag{19}$$

From the model equations (1) the new infections and transfer terms are given by,

$$f_i = \begin{bmatrix} (\sigma I_a + \delta C + \phi P)S_h \\ 0 \\ \beta P S_a \\ 0 \end{bmatrix} \tag{20}$$

and

$$v_i = \begin{bmatrix} (\mu_h + r)I_h \\ \theta C - \omega P \\ (\mu_a + \pi)I_a \\ \pi I_a - \theta C \end{bmatrix}. \tag{21}$$

Derivatives of f_i and v_i with respect to infected classes at disease free equilibrium are:

$$F = \begin{bmatrix} 0 & \sigma\frac{b_h}{mu_h} & \delta\frac{b_h}{\mu_h} & \phi\frac{b_h}{\mu_h} \\ 0 & 0 & 0 & 0 \\ 0 & \beta\frac{b_a}{\mu_a} & 0 & 0 \\ 0 & 0 & 0 & 0 \end{bmatrix} \tag{22}$$

and

$$V = \begin{bmatrix} \mu_h + r & 0 & 0 & 0 \\ 0 & -\omega & 0 & \theta \\ 0 & 0 & \mu_a + \pi & 0 \\ & 0 & 0 & \pi & -\theta \end{bmatrix}. \tag{23}$$

The inverse of the matrix V is:

$$V^{-1} = \begin{bmatrix} \frac{1}{\mu_h + r} & 0 & 0 & 0 \\ 0 & \frac{-1}{\omega} & \frac{\pi}{(\mu_a+\pi)\omega} & \frac{-1}{\omega} \\ 0 & 0 & \left(\frac{1}{\mu_a + \pi}\right) & 0 \\ 0 & 0 & \frac{\pi}{(\mu_a+\pi)\theta} & \frac{-1}{\theta} \end{bmatrix} \tag{24}$$

and the product of matrices F and V^{-1} is;

$$FV^{-1} = \begin{bmatrix} 0 & -\frac{\phi\, b_h}{\mu_h\omega} & \frac{\sigma\, b_h}{\mu_h(\mu_a+\pi)} + \frac{\delta\, b_h\pi}{\mu_h(\mu_a+\pi)\theta} + \frac{\phi\, b_h\pi}{\mu_h(\mu_a+\pi)\omega} & -\frac{\delta\, b_h}{\mu_h\theta} - \frac{\phi\, b_h}{\mu_h\omega} \\ 0 & 0 & 0 & 0 \\ 0 & -\frac{\beta\, b_a}{\omega\,\mu_a} & \frac{\pi\beta\, b_a}{\mu_a(\mu_a+\pi)\omega} & -\frac{\beta\, b_a}{\omega\,\mu_a} \\ 0 & 0 & 0 & 0 \end{bmatrix} \tag{25}$$

From (19) the basic reproduction number R_0 is given by:

$$R_0 = \frac{\beta b_a \pi}{\mu_a(\mu_a + \pi)\omega} \tag{26}$$

The basic reproduction number R_0 depends on animal infection rate β, animal recruitment rate b_a, animal anthrax induced death rate π, animal natural mortality μ_a and pathogen's natural death rate ω. The basic reproduction number R_0 is directly proportion to β and b_a therefore

increasing β and b_a will also increase the basic reproduction number R_0. Parameters μ_a and ω which are animal and pathogen's natural death rates are inversely proportional to the basic reproduction number R_0. Increasing animal and pathogens' natural death rates will decrease the basic reproduction number R_0.

3. Sensitivity Analysis

Sensitivity analysis assists to understand the potentials of each parameter to disease transmission [4]. It identifies sensitive parameters which should be the target when designing disease interventions. We employ the Maximum Likelihood estimation, an inbuilt Matlab fminsearch function to estimate our parameters.

Table shows the model parameters' values. Parameter values from the related literature were used as initial values to fit the model from the data collected from the field. The data were collected at Ngorongoro district in Tanzania from 2006 to 2016 [11].

Parameter	Values &Units	Source	Fitted Parameters
b_a	$1.369 \times 10^{-}5\ day^{-1}$	[14, 10]	0.0002
β	$0.0001\ day^{-1}$	[14, 10]	0.0016
θ	$0.001125\ day_{-1}$	[14, 10]	0.0386
ω	$0.000014\ day^{-1}$	[14, 10]	0.0003
μ_a	$0.0001\ day^{-1}$	[14, 10]	0.0006
π	0.06	assumed	0.4141
μ_h	$0.00016\ day^{-1}$	assumed	0.0002
b_h	$0.015\ day^{-1}$	assumed	0.0005
δ	$0.000002\ day^{-1}$	Assumed	0.0001
ϕ	$0.000001219\ day^{-1}$	Assumed	0.0003

4. Sensitivity Analysis of R_0

In this section parameters' indices with respect to basic reproduction number R_0 are determined. The basic reproduction number R_0 depends on five parameters which are used to derive analytical expression for each parameters. If λ is a parameter in the basic reproduction number R_0 its sensitivity index with respect to R_0 is given by:

$$r_{\lambda}^{R_0} = \frac{\partial R_0}{\partial \lambda} x \frac{R_0}{\lambda} \tag{27}$$

Using equation (27), sensitivity index for each parameter is given in Table .

Parameter	Sensitivity Index
β	$+1.0000$
b_a	$+1.00000$
π	$+0.001446829127$
μ_a	-1.001446829
ω	-1.0000

From sensitivity indices we note that, positive indices imply proportional relationship with basic reproduction number R_0. Any percentage increase in parameters with positive indices will make the same percentage increase in basic reproduction number R_0. Parameters with positive indices are animal recruitment rate b_a and animal infection rate β.

On the other hand, negative indices imply inverse relationship with basic reproduction number R_0. Any percentage increase in parameters with negative indices will make the same percentage reduction in basic reproduction number R_0. Parameters with negative sensitivity indices are animal death rate μ_a and pathogens' life span ω.

5. Numerical Simulation

In this section long and short terms behavior of anthrax dynamics in both humans and animal by considering sensitive parameter is analyzed. Parameter values from the data collected from the field are used. The general dynamics of anthrax with no controls is demonstrated in Figure 2

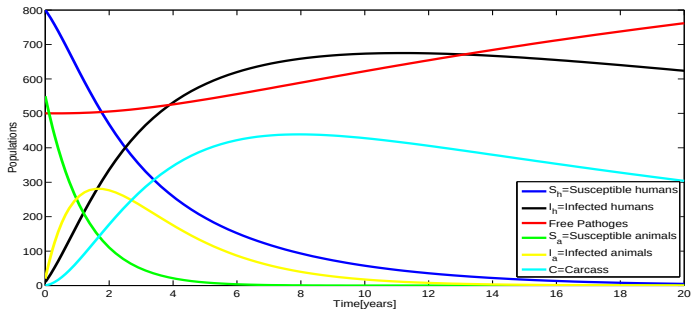

FIGURE 2. The general dynamics of anthrax in humans and animals

Susceptible humans and animals decrease due to anthrax infection rate as shown in Figure 2. Susceptible animals decrease exponentially as they acquire bacillus anthraces during grazing [3, 12]. Humans decrease as they acquire anthrax from environment or by eating meat from infected animals or by contacting infected carcasses or coming into contact with pathogen in the environment. The anthrax infection appear to be critical between five to fifteen years as demonstrated by Figure 2. However, pathogens are increasing due to shedding and decomposition of carcasses.

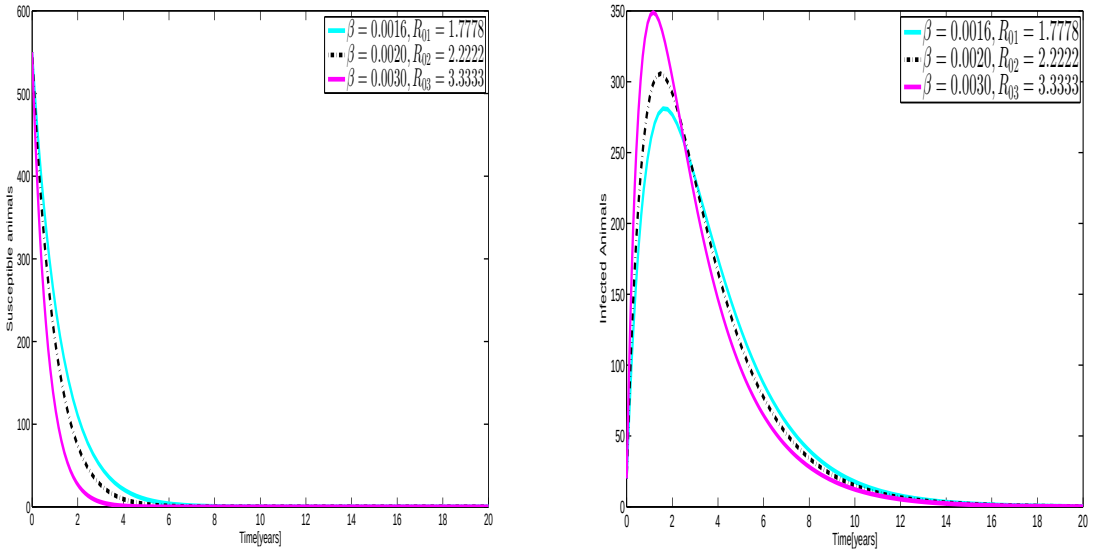

(A) Anthrax in susceptible animals (B) Anthrax in infected animals

FIGURE 3. Variation of anthrax transmission dynamics with animal infection rate

Figure 3 shows the effect of varying animal transmission rate to the dynamics of anthrax in both susceptible and infected animals. It is found that as animal infection rate increases,

susceptible animals decrease while infected animals flourish. When animals are infected at a rate 0.003 day^{-1}, all susceptible animals may acquire anthrax in twelve years as demonstrated in Figure 3a.

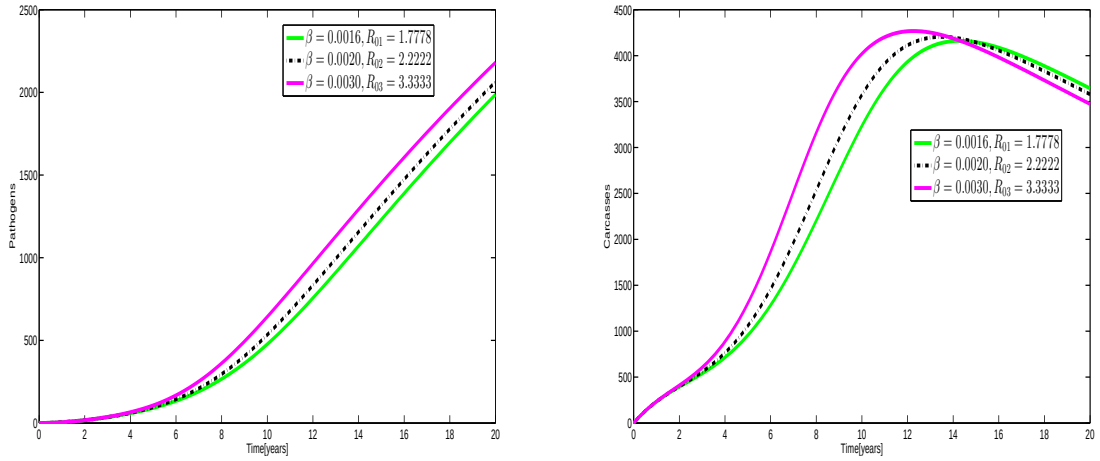

(A) Anthrax in pathogens population (B) Anthrax in carcasses population

FIGURE 4. Variation of animal infection rate in carcass and pathogen Population

Figure 4a shows the effect of varying animal transmission rate in both pathogens and carcasses population. The results show that as the animal transmission rate increases both carcasses and pathogens increase correspondingly.

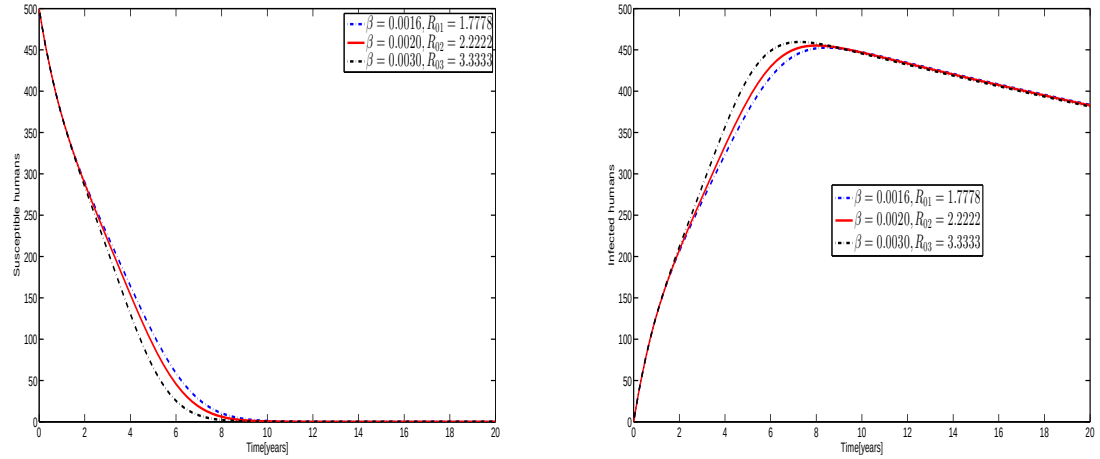

(A) Anthrax dynamics in susceptible humans population (B) Anthrax dynamics in infected humans population

FIGURE 5. Variation of animal infection rate in both susceptible and infected humans

Susceptible and infected humans are demonstrated in Figure 5. The results show that when the animal transmission rate increases, susceptible humans decrease. The rise and fall of the graph are due to the nature of the occurrence of the disease whereby the disease erupts in seasonally during the rainy and high drought period.

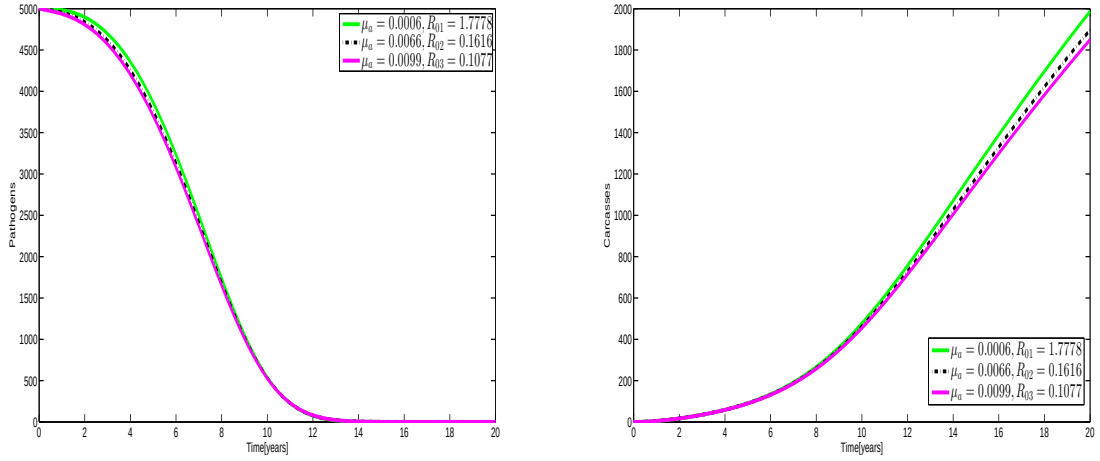

(A) Anthrax dynamics in pathogens population (B) Anthrax dynamics in carcasses population

FIGURE 6. Variation of animal natural death rate in both pathogens and carcasses

Figure 6 shows the effect of varying the animal natural death rate in both pathogens and carcasses. The results shows pathogen and carcasses decrease as animal death rate increases.

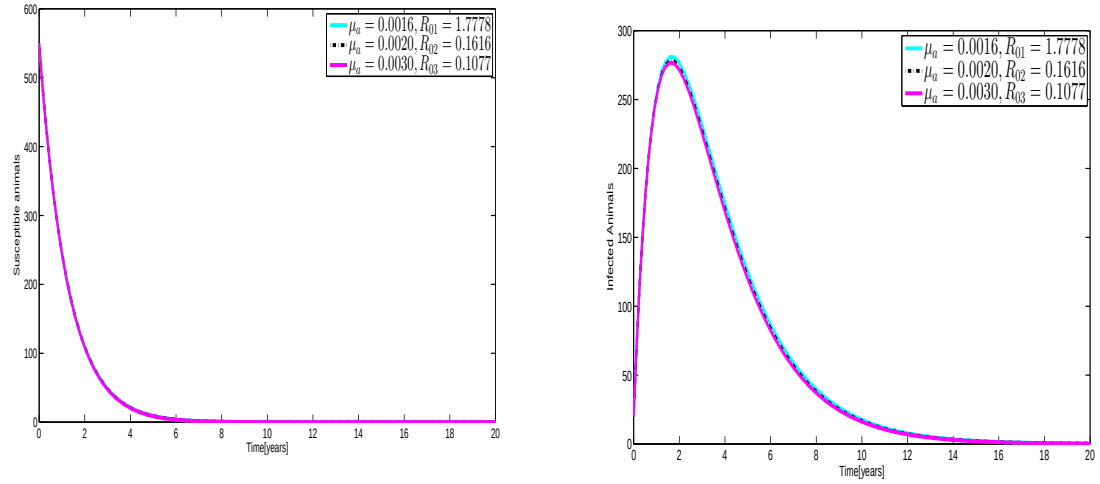

(A) Anthrax dynamics in susceptible animal population (B) Anthrax dynamics in infected animal population

FIGURE 7. Variation of animal natural death rate in both susceptible and infected animal

Figure 7 shows the effect of varying animal natural death rate in both susceptible and infected animals. The result shows that when the animal natural death rate increases both susceptible and infected animal decrease.

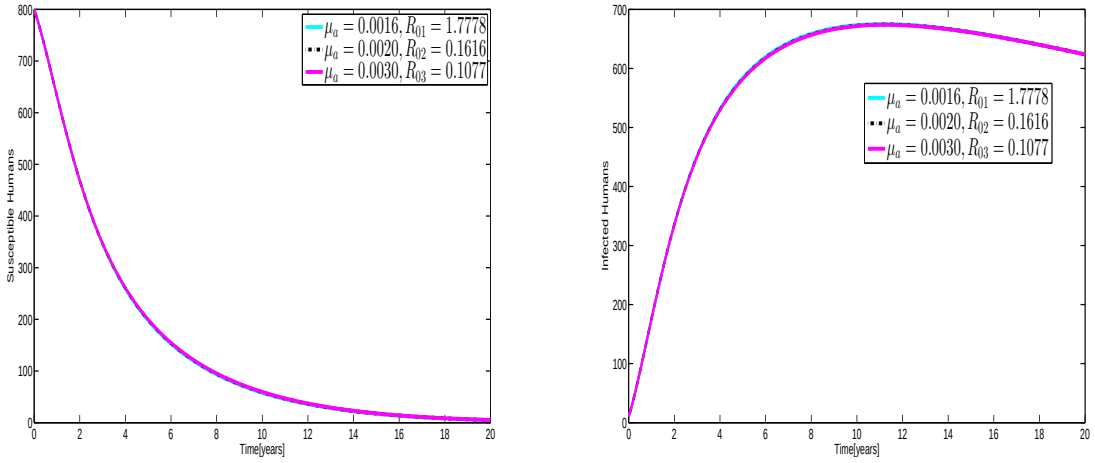

(A) Anthrax dynamics in susceptible humans population

(B) Anthrax dynamics in infected humans population

FIGURE 8. Variation of animal natural death rate in both susceptible and infected humans

Figure 8 shows the effect of varying animals natural death rate to both susceptible and infected humans. The results show that when animal natural death rate increases susceptible humane increases and infected humans decreases.

6. Conclusion, Discussion and Recommendation

A simple anthrax model in humans and animals is developed and analyzed to determine which parameters drive the transmission dynamics of the disease. The basic reproduction number R_0 is computed and sensitivity index for each parameter in the basic reproduction number R_0 is derived. The analysis shows that animal recruitment and infection rates are more sensitive to the disease transmission. Anthrax infection increases as more animals are recruited and it decreases as animals suffer natural mortality. These results are demonstrated by numerical simulation. To eradicate the disease, this study proposes control strategies such as animal vaccination, fumigation and decomposition of carcasses.

Acknowledgement

The author thanks the Nelson Mandela African Institution of Science and Technology,Germany Academic Exchange and Supervisors for their support.

Conflict of Interests

The authors declare that there is no conflict of interests.

REFERENCES

[1] O. Diekmann, J. A. P. Heesterbeek, and J. A. Metz. On the definition and the computation of the basic reproduction ratio r0 in models for infectious diseases in heterogeneous populations. J. Math. Biol., 28(4)(1990): 365382.

[2] A. Friedman and A.-A. Yakubu. Anthrax epizootic and migration: persistence or extinction. Math. Biosci., 241(1)(2013): 137144.

[3] P. Furniss and B. Hahn. A mathematical model of an anthrax epizotic in the kruger national park. Appl. Math. Model., 5(3)(1981): 130136.

[4] D. Hamby. A review of techniques for parameter sensitivity analysis of environmental models. A review of techniques for parameter sensitivity analysis of environmental models. Environ. Monitor. Assess. Monitor Assess., 32(2)(1994): 135154.

[5] R. Harrington, N. Owen-Smith, P. C. Viljoen, H. C. Biggs, D. R. Mason, and P. Funston. Establishing the causes of the roan antelope decline in the kruger national park, South Afr. Biol. Conserv., 90(1):6978, 1999.

[6] J. I. Irunde, L. S. Luboobi, and Y. Nkansah-Gyekye. Modeling the effect of tobacco smoking on the in-host dynamics of hiv/aids. J. Math. Comput. Sci., 6(3)(2016): 406-436.

[7] M. J. Keeling and P. Rohani. Modeling infectious diseases in humans and animals. Princeton University Press, 2008

[8] T. Lembo et al. Serologic surveillance of anthrax in the serengeti ecosystem, tanzania, 19962009, Emerg Infect Dis. 17(3)(2011): 387-394.

[9] M. Mourez, D. B. Lacy, K. Cunningham, R. Legmann, B. R. Sellman, J. Mogridge, and R. J. Collier. 2001: a year of major advances in anthrax toxin research. Trends Microbiol., 10(6)(2002): 287293.

[10] S. Mushayabasa, T. Marijani, and M. Masocha. Dynamical analysis and control strategies in modeling anthrax. Comput. Appl. Math., 36(3)(2017), 13331348.

[11] E. R. Mwakapeje, S. Hgset, R. Fyumagwa, H. E. Nonga, R. H. Mdegela, and E. Skjerve. Anthrax outbreaks in the humans-livestock and wildlife interface areas of northern tanzania: a retrospective record review 20062016. BMC Public Health, 18(1)(2018): 106.

[12] W. H. Organization and I. O. of Epizootics. Anthrax in humans and animals. World Health Organization, 2008.

[13] B. Raymond, K. L. Wyres, S. K. Sheppard, R. J. Ellis, and M. B. Bonsall. Environmental factors determining the epidemiology and population genetic structure of the bacillus cereus group in the field. PLoS Pathogens, 6(5)(2010): e1000905.

[14] Z. M. Sinkie and S. Narasimha Murthy. Modeling and simulation study of anthrax attack on environment. J. Multidiscip. Eng. Sci. Techn., 3(4)(2016), 4574 - 4578.

[15] P. Turnbull. Introduction: anthrax history, disease and ecology. In Anthrax, pages 119. Springer, 2002.

[16] P. Van den Driessche and J. Watmough. Reproduction numbers and sub-threshold endemic equilibria for compartmental models of disease transmission. Math. Biosci., 180(1-2)(2002): 2948.